CHALMERS

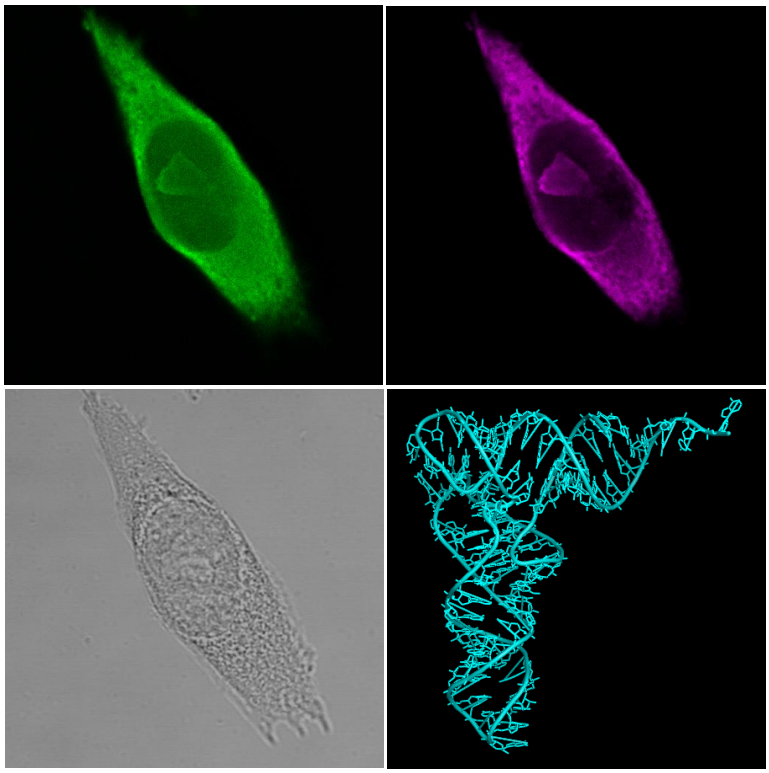

Exploring Cellular Localization and Binding Preference for Lipophilic Ruthenium Complexes

Master of Science Thesis

Maria Matson

Department of Chemical and Biological Engineering
Division of Chemistry and Biochemistry, Physical Chemistry
CHALMERS UNIVERSITY OF TECHNOLOGY
Göteborg, Sweden, 2010

THESIS FOR THE DEEGREE OF MASTER OF SCIENCE

Exploring Cellular Localization and Binding Preference for Lipophilic Ruthenium Complexes

Maria Matson

CHALMERS

Department of Chemical and Biological Engineering
CHALMERS UNIVERSITY OF TECHNOLOGY
Göteborg, Sweden 2010

Exploring Cellular Localization and Binding Preference for Lipophilic Ruthenium Complexes

Department of Chemical and Biological Engineering
Chalmers University of Technology
SE-412 96 Göteborg
Sweden

Tel. +46 (0) 31 772 10 00

Cover picture:
Top: Remarkable similarity. Fixed cells stained with the ruthenium complex D4 (green) and the RNA probe Syto RNAselect (purple). The staining pattern of D4 is very similar to the one for the RNA probe. The only difference is that the RNA probe does not stain the DNA in the nucleus.

Bottom: Transmission image of the stained cell and a three-dimensional structure of tRNA (PDB ID: 1TN2, created in PyMOL Molecular viewer)

Department of Chemical and Biological Engineering
Göteborg, Sweden 2010

Exploring Cellular Localization and Binding Preference for Lipophilic Ruthenium Complexes

Maria Matson

Department of Chemical and Biological Engineering
Chalmers University of Technology

Abstract
Ruthenium complexes have been intensively studied due to their strong DNA binding which make them interesting in the development of new DNA targeting drugs. In addition to the strong DNA binding, ruthenium dipyridophenazine complexes have shown to have exceptional photophysical properties making them highly luminescent in organic environments or bound to DNA or lipid membranes. This emission is totally quenched in aqueous solution which makes them suitable for cellular imaging with fluorescence microscopy due to the lack of background luminescence. For both applications the interaction between complexes and biomolecules is important to study and so far little is known about the RNA binding properties of ruthenium complexes.

In this thesis, three lipophilic ruthenium dppz complexes were investigated regarding their binding preference to RNA, DNA and lipid membrane as well as their intracellular localization by spectroscopy and microscopy methods. The results show that the more lipophilic complexes prefer membrane binding but also bind to RNA and DNA. In contrast the least lipophilic complex favor DNA binding but show no or very weak binding to RNA. This is further confirmed in fixed cells stained with complexes, where the more lipophilic complexes intensively stain the membrane and RNA rich cytoplasm and the least lipophilic complex dye the DNA in the nucleus. Thus a small change in lipophilicity results in varied binding preferences and cellular localization.

Keywords: Ruthenium(II) Complex, Dipyridophenazine, RNA, DNA, Membrane, Emission Spectroscopy, Confocal Laser Scanning Microscopy, Fluorescence Lifetime Imaging Microscopy.

Table of Contents

List of Abbreviations

phen	1,10-phenanthroline
dppz	dipyrido[3,2-*a*:2',3'-*c*]phenazine
D2	$[Ru(II)(phen)_2(dppzR_2)]^{2+}$, $R=CH_2OC_2H_5$
D4	$[Ru(II)(phen)_2(dppzR_2)]^{2+}$, $R=CH_2OC_4H_9$
D6	$[Ru(II)(phen)_2(dppzR_2)]^{2+}$, $R=CH_2OC_6H_{13}$
CD	Circular dichroism
LD	Linear dichroism
CLSM	Confocal laser scanning microscopy
FLIM	Fluorescence lifetime imaging microscopy
DNA	Deoxyribonucleic acid
RNA	Ribonucleic acid
ct-DNA	Calf thymus DNA
CHO-K1	A Chinese hamster ovary cell line

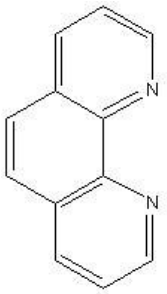

phen

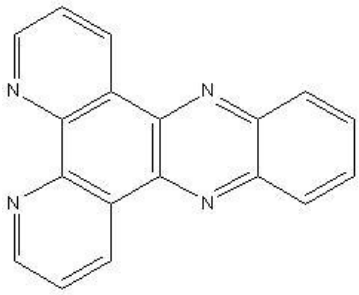

dppz

1. Introduction

Man has always been fascinated by the secrets of life. The nature of the cell is complex and there is still much that is not yet understood about the biological processes that are essential for understanding life. Insight in cellular functions is important in pharmaceutical research where the information of mechanisms and pathways can be used for understanding how diseases can be cured. DNA has for a long time been a desired drug target, especially for cancer therapeutics. The actions of these drugs are diverse but they all bind to DNA and interrupt the vital processes that occurs in the cell[1]. More recently also the endoplasmic reticulum has been suggested as a target for anti-tumor drugs. These drugs induce misfolding of proteins which eventually will lead to cell death[2]. An objective is to develop more specific drugs, for example a cancer drug only affecting the tumor[1], which would lead to more efficient drugs and reduce the side effects. In the search of the ultimate drugs, molecular interactions and biological effects are important to investigate.

In studies of biological systems visualization of cells and intracellular subunits is of great importance, which can be done with for example fluorescence microscopy. This technique requires probes, fluorescent molecules used for staining, which are selective for the desired subunit, have low background fluorescence and low photo-bleaching[3].

Various ruthenium complexes have shown to be potential therapeutic agents[4] because of the strong DNA binding, which make them function similarly to present cytostatic drugs[1, 4-9]. Complexes with dipyridophenazine (dppz) derivates as ligands have also been proposed as promising cellular probes due to their low background luminescence and tuned cellular accumulation depending on the substitution of the ligand[6, 10-11]. However, very few studies on the RNA binding properties of ruthenium complexes have been done[12-14].

In this master thesis, a series of three ruthenium(II) dppz complexes varying in lipophilicity, was investigated, see Figure 1. The purpose was to study if the complexes bind to RNA and to explore the binding preference of the complexes; comparing RNA with DNA and membranes. The cellular localization of the complexes was examined to identify in which cellular structures the complexes accumulate and if the localization could be associated with the binding preferences. The investigations of the ruthenium complexes were performed *in vitro* mainly by spectroscopy and in live and fixed cells using microscopy techniques.

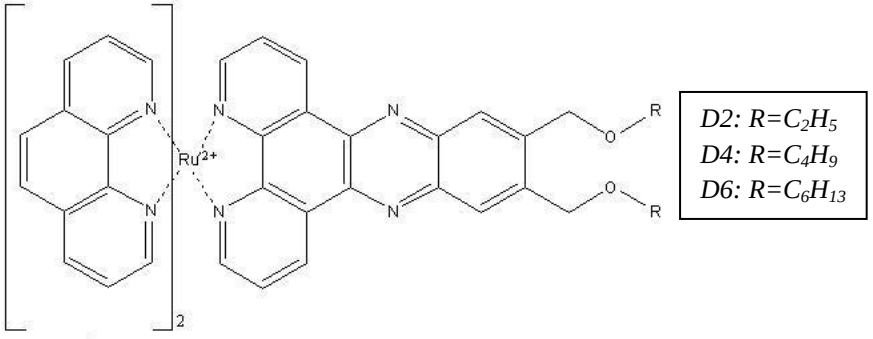

Figure 1. The three ruthenium complexes D2, D4 and D6 studied in this thesis.

2. Theory

The structure and cellular localization of nucleic acids and membranes are essential in this master thesis. The following section aims to give a brief description of these characteristics. Two mammalian cell types are used in the experiment, a cell line from hamster and neutrophilic granulocytes, white blood cells, from human. These cells are eukaryotic and therefore an overview of the eukaryotic cell is found in this chapter. Previous studies of different ruthenium complexes are presented and also theory about the used methods.

2.1 Nucleic Acids

Deoxyribonucleic acid, DNA, is the carrier of the genetic information in the cell. DNA is composed of four kinds of nucleotides arranged in a double helix of two polynucleotide chains. Each nucleotide consists of a sugar, deoxyribose, bound to a phosphate group and one of the bases adenine (A), cytosine (C), guanine (G) or thymine (T). The nucleotides are covalently bound in the strains while the two strains are held together by hydrogen bonds between the bases, called base pairing, which occurs only between A-T and C-G[15-17], see Figure 2. The sequence of the nucleotides determines the genetic information.

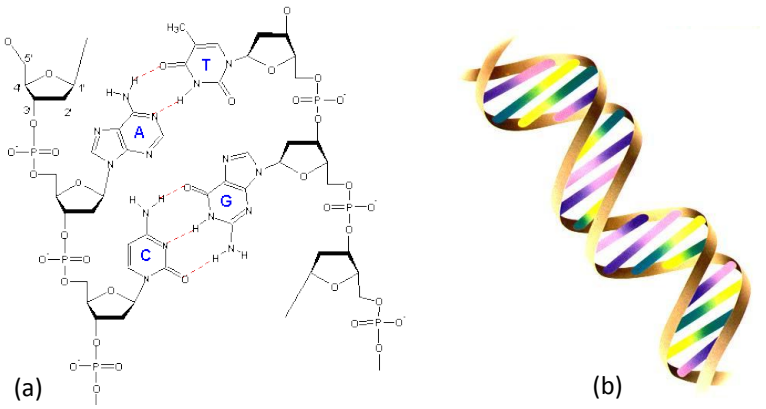

Figure 2. (a) Secondary structure and base pairing of DNA[18]. (b) The three-dimensional structure of DNA[19].

Another nucleic acid is ribonucleic acid, RNA, which subunits are very similar to DNA. The sugar of the nucleotides is ribose which has one additional hydroxyl group compared to deoxyribose, see Figure 3, and instead of the base thymine RNA has uracil (U). Despite these relatively small differences in the molecular structure, RNA is very different from DNA. DNA is often found as a double helix, usually twisted in the right handed B-form, while RNA is often a single strand formed in different conformations, for example small double stranded A-form helices or loops. There are different categories of RNA and the major types are presented in Table 1.

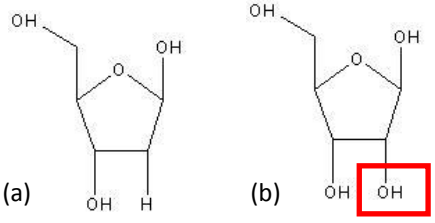

Figure 3: (a) Structure of deoxyribose. (b) Structure of ribose.

Table 1. Major types of RNA present in a eukaryotic cell

Type of RNA		Function	Percent of total RNA content in cells[15].
mRNA	Messenger RNA	Code for protein synthesis	~3-5%
tRNA	Transfer RNA	Adaptor between mRNA and amino acid.	Up to ~10%
rRNA	Ribosomal RNA	One of the compartments of a ribosome, catalysis of protein synthesis.	Up to ~80%

DNA and RNA are important in the protein synthesis in the cell which is preformed in a two step process. First the DNA sequence will be transcribed into messenger RNA, mRNA, a molecule carrying the information from the DNA to the protein factory called the ribosome and then the mRNA will be translated into a protein by the ribosome. A sequence of three nucleotides, codon, is encoding a certain amino acid carried by the tRNA with matching anti codon. The ribosome reads the mRNA and incorporates the amino acid, brought by the tRNA, into the elongated peptide chain.

The secondary structure varies between the different RNA types. mRNA is single stranded and often held linearly by proteins but when these fall off the nucleic acid fold by base pairing. tRNA is a sequence of about 80 nucleotides forming a very special structure which looks like a three-leaf clover when stretched out, see Figure 4a. Four small loops are held together of short double helical parts, forming the three leafs, and an extended small single strand, building up the stem. The three dimensional structure, however, is folded in a dense L-shaped structure. In this mode only two single stranded parts are exposed, one in each end of the L. One of these parts is the anti codon, a sequence found in of one of the loops, which functions as a recognition site in the protein synthesis. In the other end the single stranded RNA is bound to an amino acid, see Figure 4b. There are four types of eukaryotic rRNA, classified by their sedimentation factor. Together with ribosomal proteins these rRNA molecules make up the ribosomes and, additionally, rRNA also has a catalytic function in the protein synthesis. The size of all rRNA types is larger than tRNA and the structure consists of different domains of double stranded regions and loops[15-16], see Figure 4c.

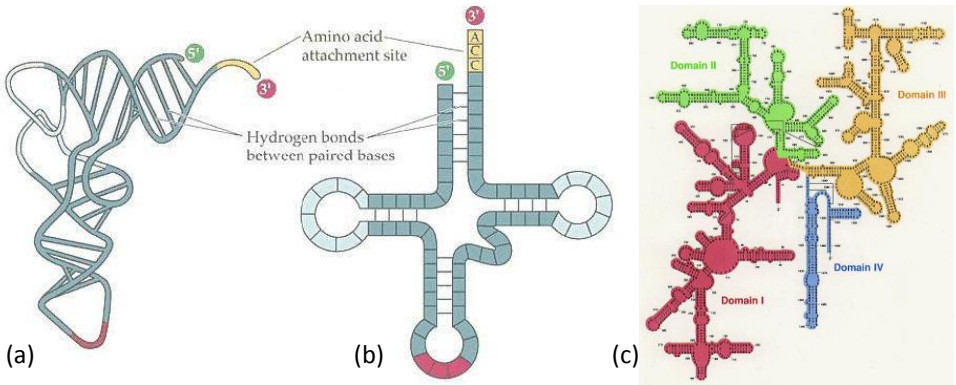

Figure 4: (a) The real three-dimensional structure of tRNA[20]. (b) The three-leaf clover secondary structure of tRNA[20]. (c) The secondary structure of one of the four rRNA types[21].

2.2 Overview of an Eukaryotic Cell

Eukaryotic cells contain a nucleus, in contrast to prokaryotic cells. The nucleus is an example of an organelle, a specialized subunit, and is the site for DNA storage and DNA/RNA synthesis. The area between the nucleus and the cell membrane is called cytoplasm and consists of the intracellular liquid called cytosol and many intracellular organelles. The separation of the nucleus from the cytoplasm is maintained by the membrane structure called nuclear envelope which is continuous with the endoplasmic reticulum, ER. The ER makes up about half of the area of the intracellular membrane structures and here the protein modification takes place. The ER functions also as an anchor for ribosomes which are attached on its cytosolic surface. The ribosomes are protein factories and millions of them are also found free in the cytoplasm. Other major organelles are mitochondria (the energy factory), the Golgi apparatus (the logistics centre), lysosome (the degrading center) and peroxisome (organelle performing oxidative reactions), see Figure 5.

Another organelle is the nucleolus which is found in the nucleus. The nucleolus is an accumulation of rRNA, ribosomal proteins and ribosomal subunits. This is where the processing of rRNA and the formation of ribosomal subunits occurs. The nucleolus has no membrane and during the cell cycle the size and number present in the cell varies depending of the requirement of ribosome synthesis. During cell division the nucleolus disassembles in order to reconstruct and grow during the rest of the cell cycle[15]. In summary, the DNA is found in the nucleus while membrane structures are found as the cell membrane, nuclear envelope and in the cytoplasm. The cytoplasm is also together with the nucleolus the location of most of the RNA types.

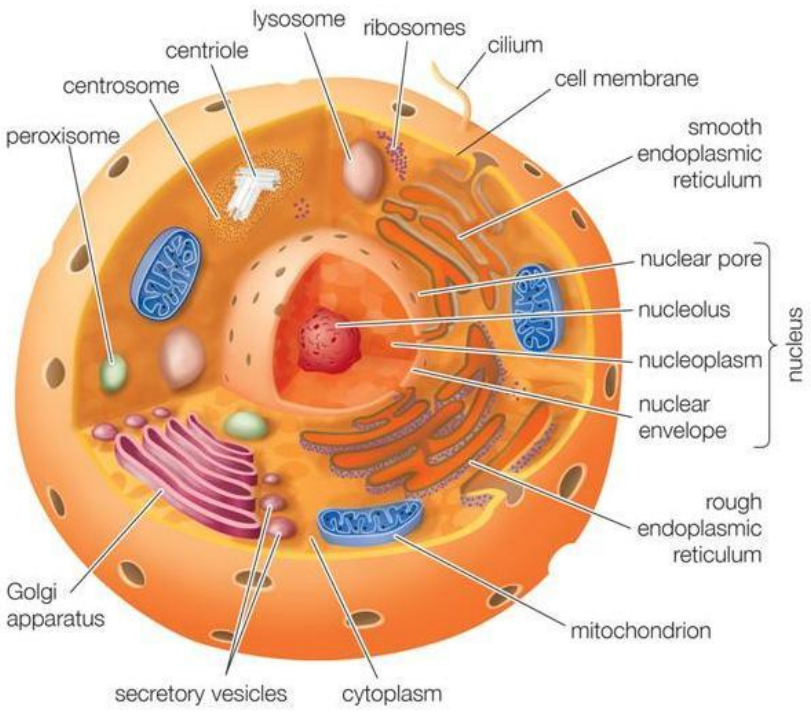

Figure 5. Drawing of a mammalian cell with organelles pointed out[22].

2.3 Membranes

Biological membranes mainly consist of lipids and proteins. The lipids are commonly phospholipids, with polar head groups and non-polar hydrocarbon chains. In aqueous solution the phospholipids arrange spontaneous into a double layer with the hydrocarbon chains internally, protected from the polar solution, while the head groups face the solution, see Figure 6. The entire cell is defined by the cell membrane but also internal organelles are surrounded by membranes. The membranes have a transport restricting function since these lipid bilayers acts as a semi permeable barrier through which only certain molecules can pass. Besides the passive diffusion of small molecules, transport across the membrane can for example occur through specialized proteins or by endocytosis. In endocytosis extracellular molecules are internalized by membrane enclosure around them, which often is induced by interaction of the molecules and proteins on the cell surface. The small membrane enclosed structures are called endosomes and these will transport known molecules to their target site or unknown to the lysosomes where degradation is performed [15-16].

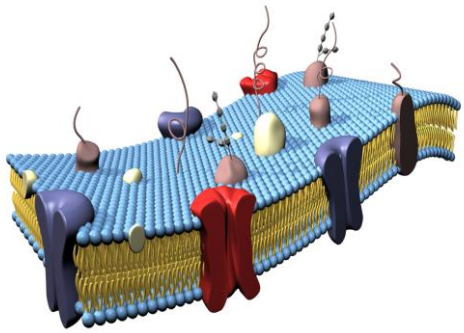

Figure 6. Drawing of a biological membrane.

2.3.1 Membrane Models

Studies of biological membranes can be difficult to perform because of their complexity due to the large variety and functions of for example membrane proteins. To be able to study the properties and the interaction with membranes, phospholipid membrane models can be used. There are different membrane models; monolayers, planar bilayers and liposomes which are used for different motives. Liposomes consist of lipid molecules arranged in bilayers which enclose a volume by forming a sphere[15, 23], see Figure 7.

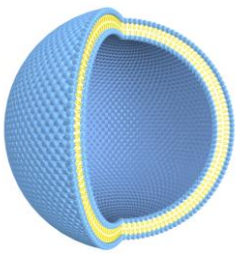

Figure 7. Drawing of a liposome, a membrane model.

2.4. Studies of Ruthenium Complexes in Biological systems

The unique photophysical properties of ruthenium complexes have been studied for a long time for different purposes[24]. Since 1984 when Burton et al. reported that $[Ru(phen)_3]^{2+}$ (phen=1,10-phenanthroline) binds to DNA by partly inserting one phen group between the base pairs of DNA, the DNA binding of ruthenium complexes has intensively been investigated[25].

By substituting one of the phen ligands with dppz the complex $[Ru(phen)_2(dppz)]^{2+}$ is obtained. This complex is found to bind even stronger to DNA than $[Ru(phen)_3]^{2+}$ by fully inserting the dppz moiety between the base pairs, a binding mode called intercalation[26-27]. This binding may interfere with fundamental cellular processes like DNA replication and transcription and eventually lead to cell death, which is the desired effect of some DNA binding drugs. Another mechanism of DNA targeting drugs is to form DNA adducts. This is the action of cisplatin and other present anticancer agents[9, 28] and has also been observed for certain ruthenium complexes after exposure to illumination[9]. Binuclear ruthenium complexes like $[\mu\text{-}(11,11'\text{-bidppz})(phen)_4Ru_2]^{4+}$ represent another type of complexes suggested as DNA targeting drugs. They have shown to bind DNA using another interesting mode, the threading intercalation, where the DNA strand has to unwind so one of the bulky structures can pass through the strand and end up on the other side. This requires a large conformational change of the helix and therefore the association and dissociation rates are very slow[29-30].

Although previously investigations have focused on the DNA binding of dppz ruthenium complexes, the complexes have also been proved to bind to lipid membranes. Unsubstituted or alkylated dppz ligands bind to the membrane by inserting the moiety parallel to the lipid hydrocarbon chains whereas nitrile and amide substituents align the dppz ligand on the surface of the membrane[11, 31]. Previous studies of the complexes studied in this thesis, show that the more lipophilic complexes prefer binding to lipid membranes compared to DNA while the opposite is true for the least lipophilic complex[10].

Cellular uptake is an important feature of molecular probes. For $[Ru(phen)_2(dppz)]^{2+}$ and similar complexes the probable uptake mechanisms have been suggested to be diffusion or endocytosis. The uptake was also shown to be higher for more lipophilic complexes presumable due to their affinity for membranes[32-33]. Another mechanism, phototoxicity, has been observed for $[Ru(phen)_3]^{2+}$ when it is exposed to an intense light source. The complex is able to penetrate the cell membrane due to formation of singlet oxygen that damages the membrane[34]. Similar to $[Ru(phen)_3]^{2+}$, the complexes investigated in this thesis also seem to permeabilize the cell membrane upon illumination and accumulate in internal structures[10].

2.5 Spectroscopy

Light, electromagnetic radiation, consists of two fields, electric and magnetic, oscillating perpendicular to each other. Interaction between molecules and light is the basis for spectroscopy.

2.5.1 Absorption Spectroscopy

Absorption is the process when molecules interacts with light and becomes excited due to that electrons are moved from the ground state to a higher electronic state. When this occurs, the charge distribution of the molecule changes in a certain direction termed transition dipole moment. The magnitude and relative orientation of the transition dipole moment is proportional to the probability for absorption.

Additionally, only radiation of a certain wavelength, λ, which corresponds to the energy gap between the states, can be absorbed. The difference in energy, ΔE, between the different states, E_1 and E_2, is given by the Bohr frequency condition

$$\Delta E = E_1 - E_2 = h\nu = \frac{hc}{\lambda} \qquad \text{eq. 1}$$

where h is Plank's constant, ν is the frequency of the electromagnetic radiation and c the speed of light.

In absorption spectroscopy a sample is illuminated by light of a defined wavelength and the incident light, I_0, and transmitted light, I, are measured. The absorption, A, is defined by the Lambert-Beer law:

$$A(\lambda) = log\frac{I_0}{I} = \varepsilon(\lambda)cl \qquad \text{eq. 2}$$

where ε is the molar extinction coefficient, l is the length that the light travelled and c is the concentration. In this thesis, the absorbance is mainly used for determination of concentrations.

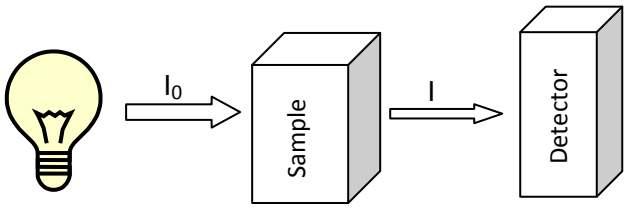

Figure 8. Schematic picture of simplified absorption spectroscopy set up. The sample is exposed to light and the difference between the incident light (I_0) and the transmitted light (I) is measured.

2.5.2 Emission Spectroscopy

From the excited state there are different pathways which can bring the molecule back to its ground state. The pathways can be non-radiative processes, where the extra energy can be released as heat, or radiative processes like fluorescence or phosphorescence, where the extra energy is released in the form of light emission. The wavelength of the emission is longer than the previously absorbed light due to that some energy is lost in non-radiative processes.

Two important properties of a fluorophore are the fluorescence quantum yield and the fluorescence lifetime. Fluorescence quantum yield is defined as the ratio between the number of emitted photons and the absorbed photons:

$$\Phi_f = \frac{k_f}{k_f + k_{nr}} \qquad \text{eq. 3}$$

where Φ_f is the fluorescence quantum yield, k_f the rate constant for the fluorescence and k_{nr} the rate constant for the non-radiative processes.

Fluorescence lifetime, τ_f, is the average time for a molecule to be in the excited state before relaxation back to the ground state. The lifetime can be calculated:

$$\tau_f = \frac{1}{k_f} \qquad \text{eq. 4}$$

In emission spectroscopy the sample is excited by a light source and the emitted light is measured. The detector is collecting the emission perpendicular to the beam from the light source to minimize detection of the excitation light. The data can the presented in a spectrum with intensity versus wavelength plotted. The emission is dependent on the structure of the fluorophore but also of the solvent[35].

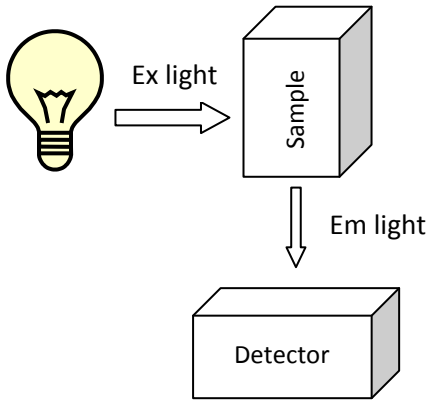

Figure 9. Schematic picture of a simplified emission spectroscopy set up. The sample is excited by a light source and the emission is detected perpendicular to the excitation direction.

2.5.3 Photophysics of Ruthenium Complexes

Ruthenium complexes with bipyridine-like ligands, for example $[Ru(phen)_2(dppz)]^{2+}$ and its derivates, forms a charge separated excited state when exposed to light. One electron is transferred to the π-orbital of the ligand from the d-orbital of the ruthenium, so called metal to ligand charge transfer. This transition can be seen as a broad absorption of light around 440nm which causes the orange color of the complex. Absorbance around 370 nm of the complex is due to an intraligand transition to an empty π orbital of the dppz ligand[27, 36-37], see Figure 10.

Ruthenium complexes with dppz moiety also possess a fascinating phenomenon called the 'light-switch' effect. When the dppz ligand is intercalated to DNA, embedded in lipid membranes or in an organic environment, the complex is strongly luminescent but in

aqueous solution the emission is totally quenched[6]. This property makes the complexes interesting as probes for cell studies using fluorescence microscopy.

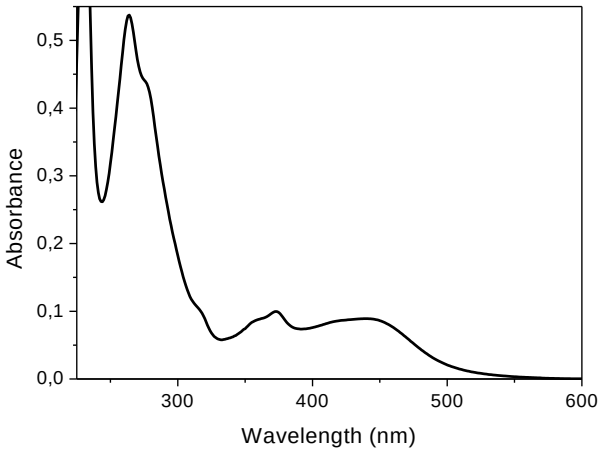

Figure 10. Absorbance spectrum of $[Ru(II)(phen)_2(dppz)]^{2+}$ in 150 mM NaCl buffer.

2.6 Polarized Spectroscopy

Polarized light can be used to gain information about molecular interactions, orientation and conformation of molecules. The light can be linearly polarized which is when the electric field of all photons in a beam are oscillating in the same plane, or circularly polarized with a helical mode of the electric field. Linear dichroism and circular dichroism are methods which both are based on difference in absorption of polarized light.

2.6.1 Circular Dichroism

Circular dichroism, CD, can be used to investigate if a sample consists of one pure enantiomer of a chiral molecule or to study a conformational change of molecules. CD is defined as the difference in absorption of left- and right circularly polarized light:

$$CD = A_l - A_r \qquad \text{eq. 5}$$

Since there must be a difference in interaction of left and right polarized light the molecules have to be chiral or arranged in a chiral way. DNA bases are achiral themselves but when arranged into a helix the polymer of nucleotides is chiral. Interaction between small achiral molecules and DNA can also be studied since they will gain an induced CD when bound to the DNA strand. A CD spectrum is commonly presented in the ellipticity unit millidegrees versus wavelength, instead of the difference in absorbance versus wavelength[38]. The conversion can be done by:

$$CD = A_l - A_r = \frac{4\pi\theta(degrees)}{180 \cdot \ln(10)} \qquad \text{eq. 6}$$

2.6.2 Linear Dichroism

Linear dichroism, LD, is defined as the difference in absorption of linearly polarized light parallel and perpendicular to the orientation axis of a molecule:

$$LD = A_{\parallel} - A_{\perp} \qquad \text{eq. 7}$$

If the transition dipole moment is oriented parallel to the orientation axis the parallel light is absorbed which will be visualized as positive LD while the opposite is true for a transition dipole moment perpendicular to the axis.

The molecules in a sample have to be oriented either by nature or by the experiment set up to achieve a LD signal. Orientation can be obtained by methods like stretched film, magnetic and electrical fields or by flow. Of these methods flow orientation is preferred for longer polymers like DNA where the viscous forces of the flow act on the polymers resulting in oriented molecules. The cylindrical couette flow cell is one kind of orientation chamber where the sample is added to a gap in between two cylinders. One cylinder is rotated in an appropriate speed to gain a significant orientation but avoiding turbulence, see Figure 11. In addition to investigation of long polymers, flow LD can also be used to study interaction of small molecules with polymers like DNA. The molecules do not orient in the flow by themselves but due to their interaction with DNA they will gain orientation. From the LD spectrum the interaction mode can be determined[38].

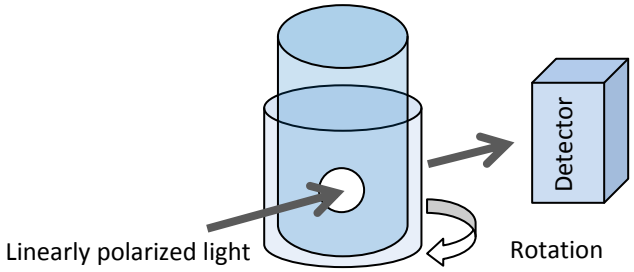

Figure 11: A drawing of a couette flow cell. A sample is applied to the space between the cylinders and one cylinder is rotated. Linearly polarized light goes through the flow cell and hit the detector.

2.7 Microscopy

Visualization of cells, organelles and intracellular processes can be done by using microscopy. There are different types of microscopy and in this thesis two techniques based on fluorescence are used; fluorescence lifetime imaging microscopy and confocal laser scanning microscopy. These methods can be used to gain information about intracellular variation of the fluorescence lifetime and the cellular localization of molecules of interest, in this thesis ruthenium(II) complexes.

2.7.1 Fluorescence Lifetime Imaging Microscopy

Fluorescence lifetime imaging microscopy, FLIM, is a method where the variation of the fluorescence lifetime for a fluorophore is studied. There are two different kinds of FLIM measurements; time-domain and frequency-domain. In time-domain measurements several images of the fluorescence intensity are collected for certain times after excitation and by varying the time delay the fluorescence lifetime for each pixel can be calculated from the images. The lifetimes are then displayed as different colors in a pseudo color map. For the frequency-domain FLIM a light source with altered intensity is used. From measurements of

the phase shift and amplitude the fluorescence lifetime can be calculated and presented in a pseudo color map.

The fluorescence lifetime depends on the environment of the fluorophore, for example the molecular binding and interactions, hydrophobic or hydrophilic properties and analyte concentrations. Since FLIM calculates the fluorescence lifetime for several positions in the sample, the variation of properties, interactions and concentrations can be examined. The method is also considered to be noninvasive and is therefore suitable for investigations of biological systems, for example intracellular processes. The technique is also used as a biomedical imaging tool for endoscopy and for studying FRET, Förster Resonance Energy Transfer, in biological systems[35, 39-40].

2.7.2 Confocal Laser Scanning Microscopy

Confocal laser scanning microscopy, CLSM, is a technique which generates very sharp images of a specific focal plane. In contrast to conventional wide field microscope which gives an average image by collecting all emitted light, CLSM selectively choose which light that reaches the detector. This is done by two lenses and a pinhole which focuses the light and exclude light which is not from the focal plane. The achieved image is a cross-section of the sample at a certain level. To get a more complete picture of the sample a 3D image can be constructed with a computer by taking cross-sections from different levels and put them on top of each other. Thus the confocal microscopy technique produces very sharp images with high resolution of a specific plane. This is useful in cell and tissue studies since dynamic processes in the internal of intact cells or tissues can be studied. However, the cells can be affected by the strong intensity of the laser and can be photo damaged[41].

2.8 Gel Electrophoresis

Gel electrophoresis is a separation method, often used for DNA, RNA or proteins. The separation takes place in a gel, consisting of a porous polymer matrix like agarose or polyacrylamide, with an applied voltage making the negatively charged molecules diffuse in a direction towards the cathode and vice versa for positively charged molecules. The separation is based on the ratio between charge and mass and all molecules with the same ratio will diffuse the same length forming a band in the gel. Smaller and/or more charged molecules diffuse faster through the gel[42]. To be able to detect the bands the gel can be stained with a fluorescent molecule, usually ethidium bromine for DNA. By comparing with a commercial available marker the size of the molecule can be determined.

3. Materials and Methods

This chapter summarizes the materials and the methods used. Experimental procedures, used reagents and the instrumentation are described and presented in this section.

3.1 Materials

The racemic mixture of the ruthenium complexes hexaflorophophates were synthesized by Minna Li as described elsewhere[10-11] and prior to the experiments these were solved in DMSO. Bovine rRNA and tRNA from *S. Cerevisiae* were purchased from Sigma Aldrich and RNA oligonucleotide (5'-CGCGUAUAUACGCG-3') and corresponding DNA oligonucleotide (5´-CGCGTATATACGCG-3´) from ATDBio. The used buffer was 150 mM NaCl, 10 mM HEPES and 1 mM EDTA dissolved in mQ-H_2O, pH 7.4.

The Chinese hamster ovarian (CHO-K1) cell line was a kind gift from Prof. Ülo Langel, Stockholm University. Cell culture reagents, fetal bovine serum, HAM's F12 medium, trypsin and L-glutamine were purchased from GTF. Neutrophilic lymphocytes purified from human blood, Bovine serum albumin (BSA) and KRG buffer (Krebs Ringer phosphate buffer) enriched with Ca^{2+} were a kind gift from Prof. Claes Dahlgren, Department of Rheumatology and Inflammation Research, Gothenburg University. The RNA probe Syto RNAselect was purchased from Molecular Probes and the membrane probe 1,6-diphenyl-1,3,5-hexatriene (DPH) from Sigma Aldrich. Enzymes, ribonucleotides, Bovine serum albumin (BSA), RNase free loading buffer and ssRNA marker (500-9000 bp) were purchased from NE Biolabs. RNase free agarose were purchased from Serva and RNase free TBE buffer from Sigma Aldrich. RNEasy mini kit and on column DNase digestion kit were purchased from Quiagen.

3.2 Spectroscopy

Additionally to the concentrations of the reagents and set up for the instruments used in the spectroscopy experiments, some information about RNA handling and how to make the liposomes are found here.

3.2.1 Working with RNA

Working with RNA requires special routines. All equipment should be RNase free why special PCR clean pipette tips (Eppendorf) and PCR clean tubes (Eppendorf) were used. The lab bench was cleaned with RNase Zap (Sigma Aldrich). RNase free water was prepared by diethyl pyrocarbonate (DEPC) treatment (1:1000) over night and autoclaving for 1 hour.

3.2.2 Preparation of liposomes

DOPG (1,2-dioleoyl-sn-glycero-3-phosphoglycerol dissolved in chloroform) 20mg/mL (79,5 µL, 2µmol) and DOPC (1,2-dioleoyl-sn-glycero-3-phosphocholine dissolved in chloroform) 25mg/mL (252µL, 8µmol) were added to a round bottom flask (this yields liposomes with 20% surface charge which corresponds to the charge of the nucleotides in the experiments). The solution was dried in a rotary evaporator for 15 minutes. The formed film was then dried further *in vacuo* for 2h. The film was dispersed in 1mL NaCl buffer (150 mM) to obtain a 10

mM solution of liposomes. To get a uniform size of the liposomes the solution was frozen with liquid nitrogen and thawed at 37˚C five times, the fifth thawing was done in room temperature, and then extruded 21 times through two polycarbonate filter with a pore size of 100 nm using a syringe LiposoFast-Pneumatic extruder (Avestin, Canada).

3.2.3 Absorption Spectroscopy

Absorption of the complexes was measured with a Cary 4000 or Cary 5000 UV-vis Spectrophotometer (Varian, USA). The spectra were recorded between 200-600 nm and the molar extinction coefficients used for concentrations determination are presented in Table 2. The rRNA and tRNA concentration was determined by comparing the absorption to a DNA sample with known concentration. The concentrations of the stem solutions were determined with a Nanodrop Spectrophotometer (Thermo Scientific, USA).

Table 2. Molar extinction coefficients

Molecule	λ (nm)	ε ($M^{-1}cm^{-1}$)
dppz, D2, D4, D6	440	20 000
ct-DNA (per base)	260	6600
DNA oligonucleotide[a]	260	147900
RNA oligonucleotide[b]	260	111605

[a] The molar extinction coefficient was supplied from BioLabs. [b] The molar extinction coefficient was calculated by using Oligoanalyzer 3.1[43], 15% was subtracted to compensate for the double stranded RNA.

3.2.4 Emission Spectroscopy

Steady state emission measurements were done with a Cary Eclipse Fluorescence Spectrophotometer (Varian, USA) at room temperature. The ruthenium complexes were dissolved to a final concentration of 2 µM and the complexes were added to tRNA/rRNA (40 µM nucleotides), DNA or RNA oligonucleotide (2µM), calf thymus DNA (40 µM nucleotides) or liposomes (200 µM). The complexes were excited at 440 nm and the emission was recorded between 550-800 nm. The spectra were normalized by the absorbance of the complexes at 440 nm.

3.2.5 CD

CD was recorded with a Chirascan CD spectrometer (AppliedPhotophysics, UK). The wavelength interval was 200-600 nm, band width 1 nm with steps of 1.0 nm. The time-per-point was 0.5 s. 100 µM DNA or RNA and 10 µM complex was used.

3.2.6 LD

LD was measured with a rebuilt Chirascan CD spectrometer (AppliedPhotophysics, UK) which uses linearly polarized light. Orientation of the samples was achieved by using a couette flow cell with an outer rotating cylinder. Rotation of 1000 RPM was used and baseline correction was done by subtracting the spectrum recorded at 0 RPM. LD spectra were recorded between 200-600 nm with 1 nm of band width and steps of 1.0 nm. The time-per-point was

0.5 s and the used concentrations were 100 µM DNA or RNA and 10 µM complex.

3.3 Gel electrophoresis

A 1% agarose gel was prepared (RNase free for RNA gels) by dissolving agarose in 1xTBE buffer (Tris 50 mM, boric acid 50 mM and EDTA 1.25 mM) under heating and stirring. The clear liquid was then cooled to 60˚C and poured out on a gel plate. A comb was placed in the upper part of the gel and the gel was left for at least 30 minutes.

The DNA was mixed with loading buffer (0.25% Bromophenol blue, 0.25% Xylene cyanol and 15% Ficoll, type 400 Pharmacia) and RNA was mixed with 2x RNase free loading buffer (2X 0.02% Bromophenol Blue, 26% ficoll (w/v), 14M urea, 4 mM EDTA, 180 mM Tris-borate) and prior to the loading of the gel, the complexes were added. The gel electrophoresis was run in 1xTBE buffer at room temperature and 5V during 1 hour using an Electrophoresis Power Supply EPS 600 (Pharmacia).

The gels were scanned with Typhoon 9410 Variable Mode Imager with Typhoon Blue Laser Module (GE Healthcare, England) to detect the complex (excitation at 488 nm and emission filter 610 nm) and after 30 minutes of staining detection of the nucleic acids were performed. For DNA detection Ethidium bromine, EtBr, (1 µg/mL) was used as dye (excitation 525 nm and emission filter 610 nm) and for RNA detection CYBR Green II (1:10000) was used (excitation 488 nm and emission filter 526). The gels were scanned with normal sensitivity, focal plane +3 mm, PMT at 600 V and with 100 µm pixel size.

3.4 *In vitro* transcription

To each sample 5.6 µL DNA (linearized T7luc-plasmid, 2,7mM), 5 µL 10X reaction buffer. 1 µL T7 RNA-polymerase (50 u/µl), 1.25 µL RNase inhibitor (1 u/µL), 0.31 µL NTP:s (80 mM of each), 0.5 µL BSA (10 g/l) and 36.94 µL DEPC-treated mQ-H_2O was added. Additional, 2 µL of 150 µM dppz complex solution (6 µM) or H_2O was added to gain 50 µL reaction volume. The transcription was done for 2 hours in 37˚C. 3µL of each sample was removed for gel electrophoresis of unpurified sample. The RNA in each sample was purified by RNAEasy with on-column DNA digestion (Quiagen, Germany), according to the protocol. The weight of the purified RNA solved in RNase free mQ-H_2O was measured and the volume of the sample was measured before an aliquot of 3 µL were removed. The aliquots prior and posture of purification were diluted with loading buffer and H_2O and denaturated at 55˚C for 15 minutes and analyzed by gel electrophoresis (see chapter 3.3. Gel electrophoresis). The RNA concentration was measured on a Nanodrop Spectrophotometer (Thermo Scientific, USA), and the amount of RNA was calculated.

3.5 Cell Studies

CHO-K1 cells were grown in HAM's F12 medium with 10% fetal calf serum and L-glutamine (2mM) at 37˚C and 5% CO_2. Twice a week the cells were trypsinated, during 5 minutes to make them loose from the growth surface, and seeded with ~7500 cells/cm^2. For CLSM and

FLIM, the cells were seeded on round coverslips with ~60 000-100 000 cells per coverslip and cultured for 2 days. For CLSM, fixation of cells were done by incubation of the cells in cold methanol (-20°C) for at least 10 minutes. The complexes were diluted to 10µM concentration in serum free media, RNA probe Syto RNAselect to 1 µM and membrane probe DPH to 20 µM. The solution was added to the solution chamber. The concentration of DMSO was not higher than 1% v/v. Longer incubation of cells with ruthenium complexes (5µM) were done during 24 hour, these cells were rinsed once and mounted in the chamber with fresh serum-free media. Prior to confocal imaging on neutrophils the coverslip was incubated with 1% BSA solution. The neutrophils were added to the solution chamber and then the ruthenium complexes, diluted in KRG buffer (2 µM).

For FLIM the coverslips were kept in the incubation dishes and the cells were methanol fixed (-20°C) for 15 minutes and rinsed once before adding complex (10 µM) in medium. Live cells were rinsed once and complex (20 µM) in serum-free medium was added.

3.5.1 CLSM

Fluorescence images were obtained with a confocal laser scanning microscopy system (Leica TCS SP2 RS, Wetzlar, Germany) using a PL APO 63x/1.32 objective. For excitation of the ruthenium complexes and the RNA probe Syto RNAselect an Ar-laser (488nm) was used and for the membrane probe DPH a UV-laser (351nm) was used. The emission of the complexes was detected at 660-700 nm, Syto RNAselect at 520-540 nm and DPH at 370-470 nm. The PMT was varied to gain as good images as possible.

3.5.2 FLIM

Imaging of the fluorescence lifetime were performed with a Olympus IX70 (Olympus Corporation, Japan) supplemented with LIFA Fluorescence lifetime signal generator and LI^2 CAM MD camera (Lambert Instruments, Netherlands) using a LUCPlanDLN 40x/0.60 Pn2, ∞/0-2/FN22 objective. Excitation of the ruthenium complexes was done with a 405 nm diode. $[Ru(II)(phen)_2(dppz(CH_3)_2)]^{2+}$ in 1,3-propanediol (with lifetime of 192 ns) was used as reference and the modulation frequency was set to 1 MHz The exposure time for the CCP-camera and the voltage of the multichannel plate (MCP) was varied to gain as good signal as possible. Number of phase pictures was set to 12, average image to 4, reference filter size to 9 pixels and cut-off for fluorescence intensity was 20-100%. Cathode DC was -1.2 mA, cathode AC was -16.5 dbm, LED DC 100 mA and LED AC 0.5 V. A snapshot was done to gain the fluorescence intensity image of the selected area for FLIM measurements.

3.5.3 Cytotoxicity

Cells were grown in a 96 well plate and incubated with D6 during 4 hours in five different concentrations; 0.1, 1, 5, 10 and 20 µM, with three replicates of each concentration. As a control that the cells were not affected by DMSO, 2% v/v DMSO was used. Positive and negative control was live cells respective cells lysed with 1% Triton X-100. Cytotoxicity Detection Kit^{PLUS} (LDH), Roche, was used to detect the cytotoxicity.

4. Results

The results of the experiments are presented in the following section. Binding and binding preference were studied by spectroscopy while the cellular localization and uptake of the complexes was visualized by CLSM. FLIM was used to examine the intracellular variation of the fluorescence lifetime and the effect of complexes on transcription was studied by *in vitro* transcription. The strength of the DNA and RNA binding were examined by gel electrophoresis.

4.1 Spectroscopy

Emission spectroscopy measurements were done to examine RNA binding and binding preferences; comparing RNA with DNA and liposomes. This can be done due to that the emission spectra of the complexes differ depending on the surroundings. By linear and circular dichroism the binding mode of the complexes was investigated.

4.1.1 Emission spectroscopy

Three different types of RNA were used in the emission spectroscopy experiments; tRNA, rRNA and a 14 base pair long RNA oligonucleotide. The RNA oligonucleotide was compared with the corresponding DNA oligonucleotide and tRNA and rRNA was compared with ct-DNA. For all kinds of RNA a similar result was achieved.

In Figure 12 the spectra of the complexes in DNA, rRNA and liposome are presented. The intensity and the wavelength of the emission maximum varies due to the different environments of the complexes, see Table 3 for the emission maximum wavelength. D2 and D4 have high emission in DNA while the emission in rRNA is much lower. For D6 the highest emission is found in liposomes and the lower intensity of the complex in DNA and rRNA is approximately equal but the wavelength differs for the complex in the two nucleic acids.

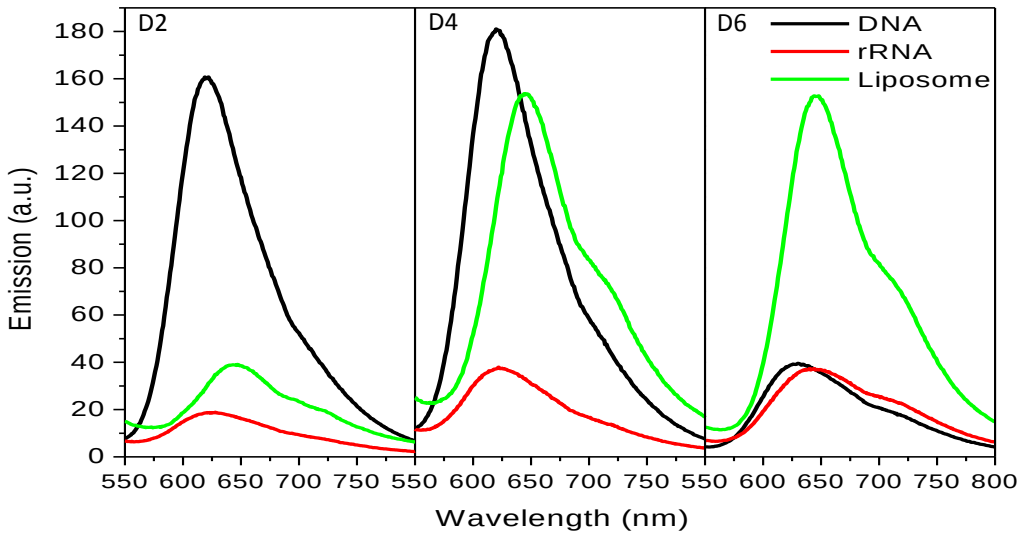

Figure 12. Emission spectra for the complexes (2µM) in DNA (40 µM bases), rRNA (40 µM bases) and liposome (200 µM).

Table 3. The emission maximum wavelengths in Figure 12.

Complex	DNA	rRNA	Liposome
D2	620 nm	625 nm	645 nm
D4	620 nm	623 nm	645 nm
D6	626 nm	642 nm	645 nm

The complexes also show different spectral properties for the different RNA types and the highest emission of all complexes is found in rRNA. D6 and D4 in rRNA have similar intensity but in tRNA and RNA oligonucleotide the signal for D4 is weaker, see Figure 13. The wavelength of the emission maximum is also shifted for the complexes in different RNA types, see Table 4.

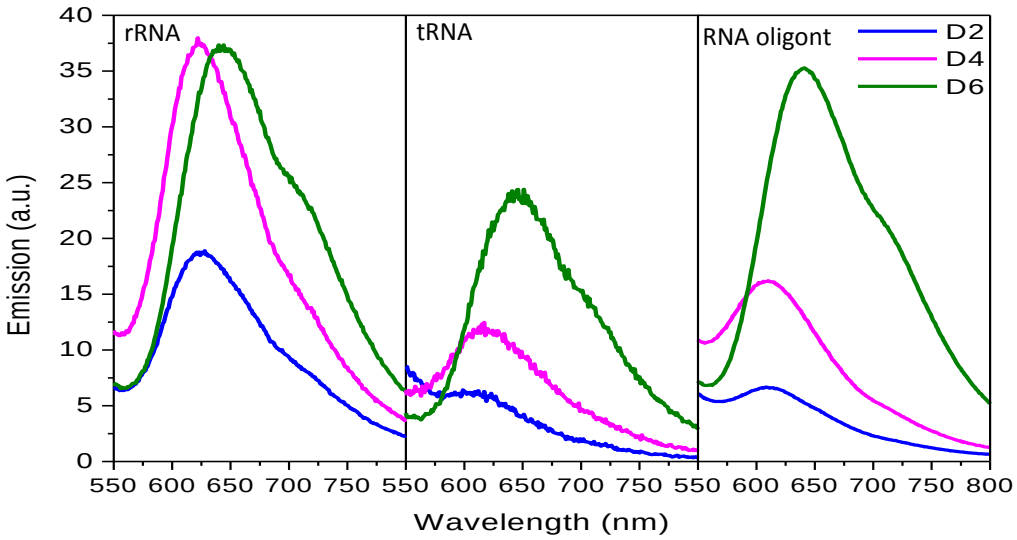

Figure 13. Emission of the complexes (2 µ M) in the different types of RNA; rRNA (40 µM bases), tRNA (40 µM bases) and RNA oligonucleotide (2 µM oligonucleotide).

Table 4. The emission maximum wavelengths in Figure 13.

Complex	rRNA	tRNA	RNA oligont
D2	625 nm	608 nm	610 nm
D4	623 nm	617 nm	611 nm
D6	642 nm	644 nm	640 nm

To examine the favored binding of a complex, the emission maximum wavelength and the intensity in mixed samples were compared to the spectra in pure DNA, rRNA and liposome seen in Figure 12. For example the emission of D6 in liposomes did not change in intensity or wavelength when rRNA was added. Thus, this complex shows preference binding to liposomes. In contrast the emission of D6 in DNA changed to lower intensity and longer wavelength (637 nm) after addition of rRNA. This indicates a mixture of DNA and rRNA binding of the complex since the emission maximum wavelength is in between the ones for

the pure nucleic acids. D6 binds stronger to rRNA than to DNA since no spectral changes were observed after addition of DNA, see Figure 14. For tRNA and RNA oligonucleotide, both RNA and DNA binding of the complex were found for the mixed samples (not shown).

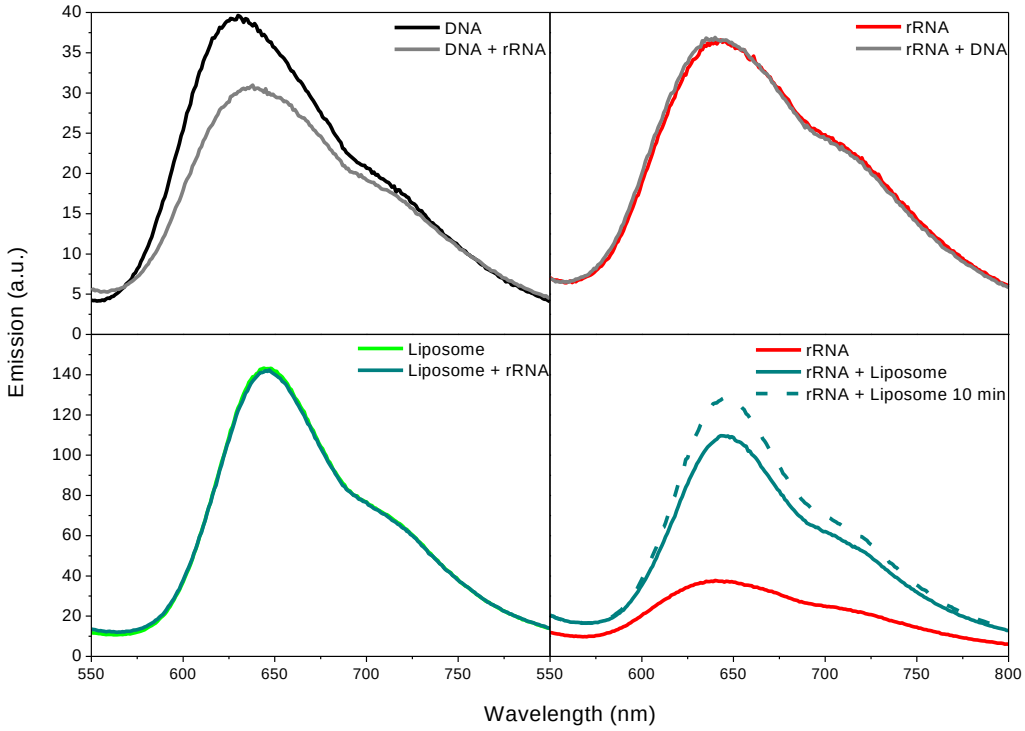

Figure 14. Emission spectra of D2 (2 µM) in pure DNA (40 µM bases,) rRNA (40 µM bases) or liposome (200 µM) and the spectral change upon addition of rRNA, DNA or liposomes are displayed. Bottom right, the change after 10 minutes is also included; this change was not significant for the other samples.

Note that D2 and D4 show no emission in buffer while D6 is luminescent in this high concentration of salt. The emission in a buffer with low salt concentration is negligible. All spectra are normalized due to the absorbance of the complex at 440 nm but note that dilution effects could not be included in the normalization of the spectra.

An overview of the results of the emission spectroscopy experiments in rRNA is presented in Table 5. The spectra of D2 and D4 corresponding to Figure 14 is found in Appendix.

Table 5. Overview of the results from the emission spectroscopy experiments with rRNA.

	D2	D4	D6
Prefers binding to	DNA	Membrane	Membrane
Binds to rRNA	(+)	+	++
Prefers DNA or rRNA	DNA	DNA	rRNA
Prefers Membrane or rRNA	Membrane	Membrane	Membrane

4.1.2 LD

LD measurements were done for the three complexes and for the well-known intercalator $[Ru(phen)_2(dppz)]^{2+}$. The negative signal for DNA at 260 nm, seen in Figure 15, origins from the DNA bases which are perpendicular to the orientation axis. Upon addition of complexes this signal decreases and the complexes also give rise to peaks between 340-550 nm. These signals show that the complexes are bound to DNA since orientation of the small molecules has been achieved. Although the signal is of different magnitude, increasing with decreasing lipophilicity, the pattern is similar which indicates the same binding mode to DNA, intercalation. The signal of D6 is very small but the pattern is similar to the dppz complex except from the missing phenanthroline peak at 265 nm. Control experiments done in low salt concentration display that D6 has a similar spectrum as seen for the dppz complex (data not shown).

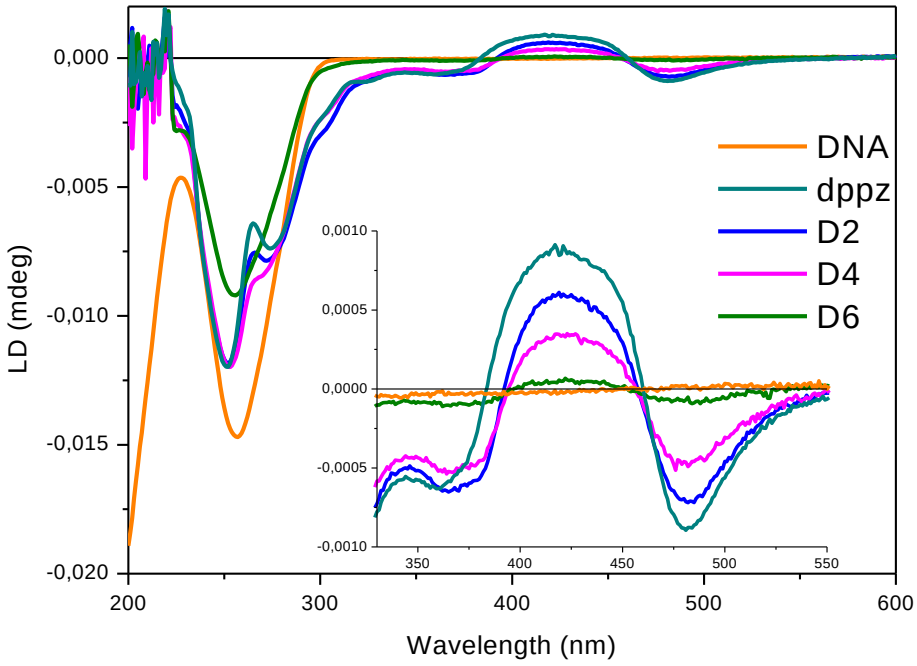

Figure 15. LD spectra of the complexes (10 µM) in DNA (100 µM) and an enlargement of the area 330-550 nm.

The corresponding experiment with RNA was not possible to perform since the different types of RNA were too short and could not be oriented in the flow cell.

4.1.3 CD

DNA and tRNA binding were investigated with CD spectroscopy. If the complexes bind to the nucleic acids they gain an induced CD since they are arranged in a chiral way. This can be displayed in a spectrum by subtracting the pure DNA or RNA signal from the spectra where the complexes are added. As seen in Figure 16 (a) the induced CD for the different complexes in DNA has the same pattern as for the dppz complex but the magnitude differs

between the complexes. The weakest signal is obtained from D6 and the signal seems to increase for decreasing lipophilicity of the complex.

In tRNA the induced CD signals of the complexes are weak. The spectrum in Figure 16 (b) indicates that D6 binds best to tRNA of the three complexes.

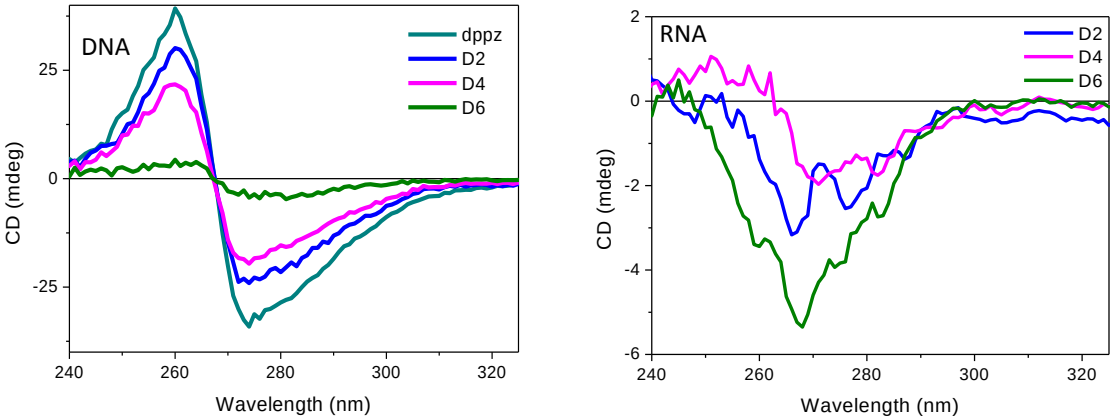

Figure 16. Induced CD of the complexes (10 µM) in (a) DNA (100 µM) and (b) RNA (100 µM)

4.2 Gel electrophoresis

Gel electrophoresis was performed to investigate if the binding of the complexes was strong enough for the complexes to migrate together with DNA or RNA in the gel. Since the complexes themselves are positively charged, only strongly bound complex would migrate through the gel in the same direction as the negatively charged nucleic acids. In the gel with complex bound to DNA, the complexes dppz, D2 and D4 migrated with the DNA whereas D6 did not, see Figure 17 (a). This was also seen immediately on the gel by naked eye since the complexes appeared as yellow bands. The DNA was also observed to migrate different lengths where DNA with dppz complex and D2 migrated shortest path, see Figure 17 (b).

(a)

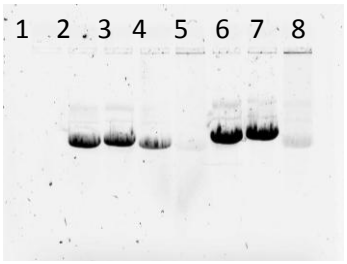

(b)

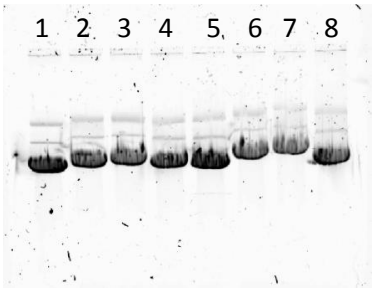

Well	Content	Ratio
1	Pure DNA	-
2	DNA + dppz	1:12
3	DNA + D2	1:12
4	DNA + D4	1:12
5	DNA + D6	1:12
6	DNA + dppz	1:6
7	DNA + D2	1:6
8	DNA + D6	1:6

Figure 17. Gel with DNA and complex. (a) The emission of the complexes (b) DNA bands visualized by EtBr staining. The ratio in the description refers to complex:base pair.

The corresponding experiment with RNA was done with both rRNA and tRNA and no yellow bands were observed on the gel. Prior to staining, emission at the same position in all wells were seen, even for the pure RNA samples, see Figure 18 (a), which probably is due to something fluorescence in the loading buffer. In Figure 18 (b) the different RNA types are detected on different positions at the gel, rRNA has migrated shorter length than tRNA.

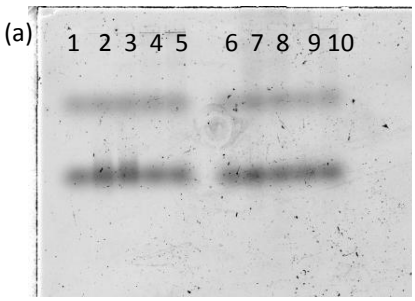

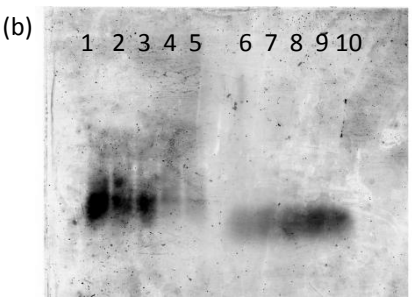

Well	Content
1	rRNA
2	rRNA + dppz
3	rRNA + D2
4	rRNA + D4
5	rRNA + D6
6	tRNA
7	tRNA + dppz
8	tRNA + D2
9	tRNA + D4
10	tRNA + D6

Figure 18. Gel with RNA and complex. (a) Prior to staining, emission is seen in every well. (b) RNA bands visualized by CYBR Green II staining.

4.3 *In vitro* Transcription

The result from the *in vitro* transcription experiments shows that the dppz complex affects the transcription of DNA. The amount of RNA produced by the enzymes was lower than the control sample containing DNA without complex, see Figure 19.

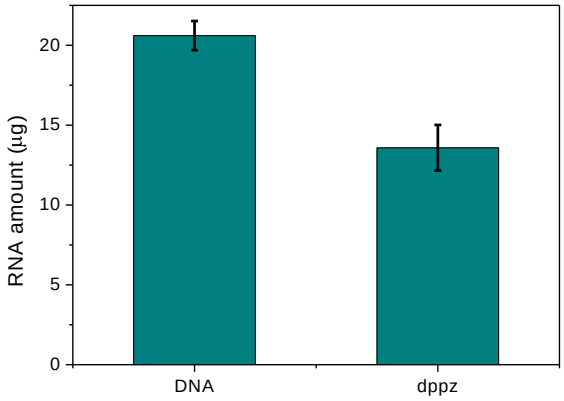

Figure 19. Amount RNA produced in the in vitro transcription experiments with and without dppz complex added to DNA.

4.4 Confocal Laser Scanning Microscopy

To investigate the cellular localization of the complexes fixed cells were used. The membranes of these cells are permeabilized and thus the complexes can freely enter and accumulate in their favored intracellular structures. The obtained images show that the complexes differ in cellular staining, D6 is found in the cytoplasm while D2 is in the nucleus. D4 is located both in the cytoplasm and the nucleolus and also in the nucleus, although the emission is not as intense in the nucleus. The localization of complexes was compared with the RNA probe Syto RNAselect, which has about 10 times higher emission in RNA compared to DNA. The probe stains the cytoplasm and the rRNA rich nucleolus which is a pattern very similar to D4 dyeing, except for the nuclear staining of D4. D6 also have similar pattern but do not stain the nucleolus while D2 stains the opposite compartments comparing to the probe, see Figure 20.

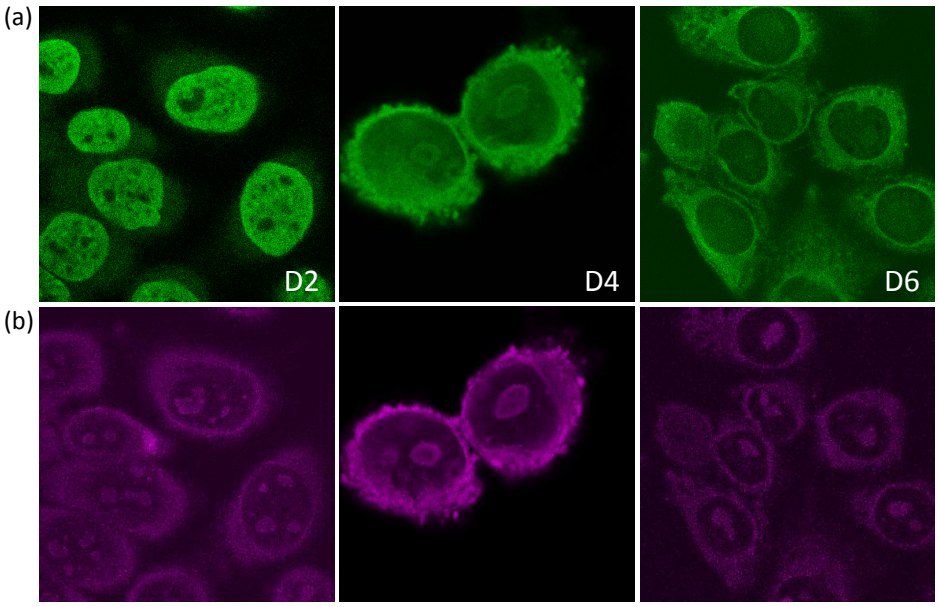

Figure 20. Fixed cells stained with (a) the different complexes (10µM). (b) RNA probe Syto RNAselect (1 µM).

To further investigate the cellular accumulation of the complexes, fixed cells were also stained with a membrane probe, DPH, see Figure 21. The dppz complex was also investigated which stains the nucleus similar to D2. The membrane probe turned out to not give any detailed information but the staining is clearly more intense in the cytoplasm and the nuclear envelope is distinctly visualized. In the dyeing of D6 and D4, which have similar cellular localization, the nuclear envelope is also clearly seen. Note also that the sample with D6 contained a lot of loose unknown membrane structures stained by the membrane probe. The membrane probe showed to be very sensitive and was photo bleached after a few minutes.

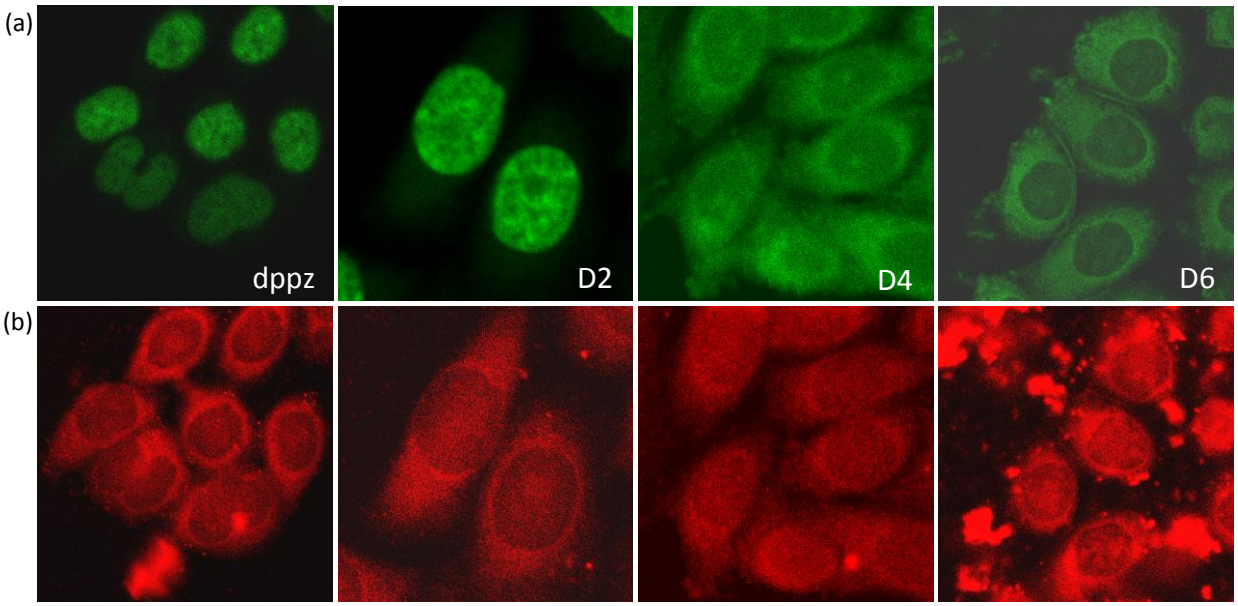

Figure 21. Fixed cells stained with (a) complex (10 µM, (b) membrane probe, DPH (20 µM).

4.5 FLIM

The complexes also differ in the color map obtained by FLIM. In each pixel of the images the fluorescence lifetime is calculated and displayed as different colors depending on the lifetime where blue is short and red long lifetimes. Comparison of the complexes can be done using the same time scale, see Figure 22. The two more lipophilic complexes have shorter lifetimes and stain the entire cells while D2 has more of longer lifetimes. Even longer lifetimes are obtained with dppz complex which is found only in the nucleus.

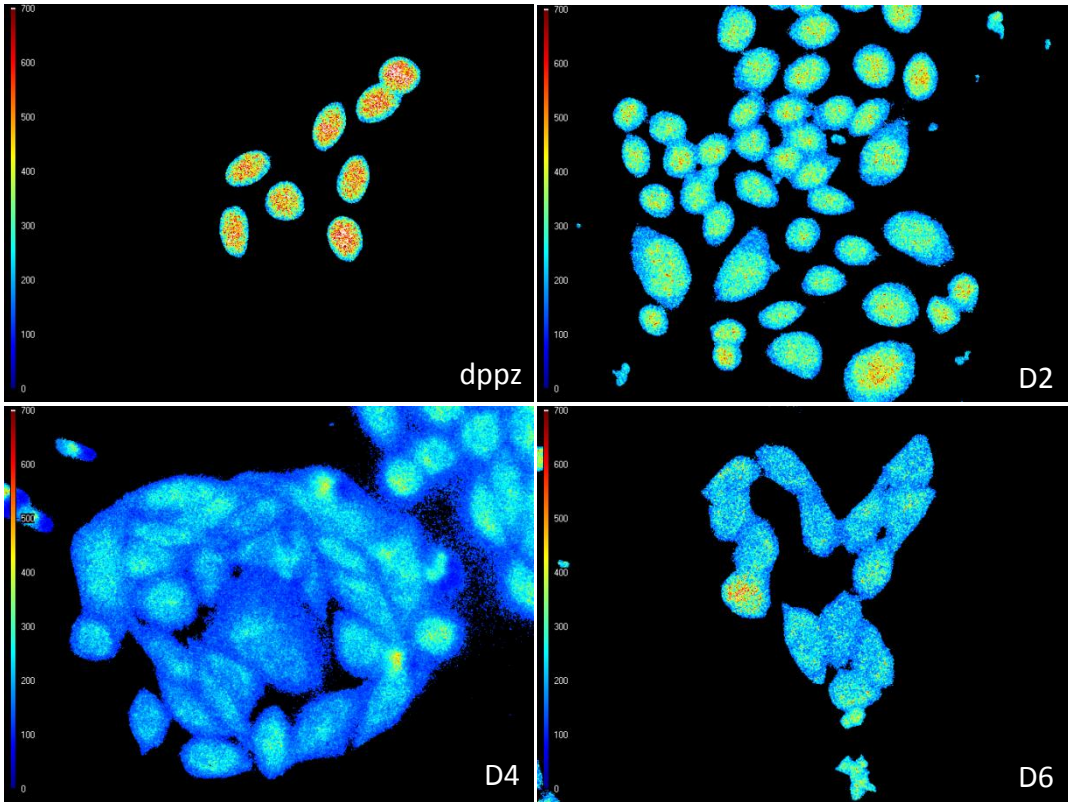

Figure 22. FLIM images of fixed cells stained with complexes (10 µM). The images have the same time scale 0-700 nm.

By using an optimal time scale, the intracellular variation of the lifetime can be further studied. As seen for D4 in Figure 23, the lifetime varies depending on the cellular localization of the complex but is not depending on the intensity of the emission. The lifetime seems to be shortest in the cell membrane and in the cytoplasm whereas the nucleus has the longest.

Nanosecond emission decays for the complexes in solutions of DNA, RNA and liposomes were measured with a Nd:YAG laser at an excitation wavelength of 440 nm. Preliminary results from these experiments show that the lifetime for complexes bound to DNA is about 400-500 ns while liposome bound complexes display lifetimes around 150-200 ns and in RNA just a few ns.

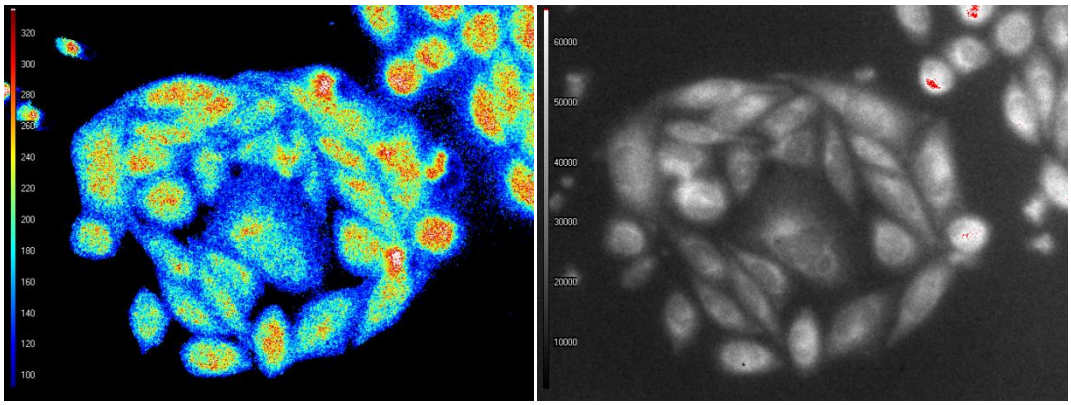

Figure 23. Fixed cells stained with D4. Left: FLIM image, right: fluorescence image.

FLIM measurements were also performed on live cells stained with D6. The obtained image has distinct yellow-red circles, indicating a lifetime around 320-380ns, which correspond to the membrane dying of the complex, see Figure 24.

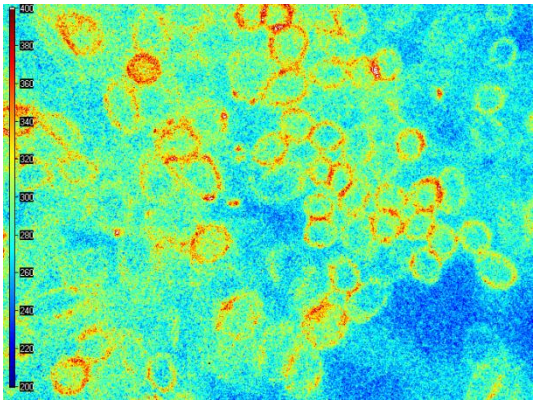

Figure 24. FLIM image of live cells stained with D6 (20 µM).

4.6 Cellular Uptake of Ruthenium Complexes

Cellular uptake of the complexes is also important to investigate if the aimed applications of the substance are probes for cellular imaging or therapeutics. When live cells are incubated for 24 hours, uptake of the complexes occur and is seen as small punctuate structures in the cytoplasm. The more lipophilic complexes, D4 and D6 seem to have a larger uptake, see Figure 25 (a). Dark incubated cells appear to be vital, judging from their normal shape, despite the presence of the complexes. This was further confirmed by a cytotoxicity test where the vitality of cells, incubated for four hours with concentrations up to 20 µM, was investigated and the cells were found to be vital.

Previous studies have shown that these complexes are able to traverse the cell membrane upon illumination, called photoactivated uptake[10]. Here, the complexes are similarly released from the intracellular vesicles of the incubated cells and spread out in the cytoplasm. In Figure 25 (b), this is shown for D6 which stains part of the cytoplasm, the nuclear envelope and the cell membrane, after 10 minutes of illumination.

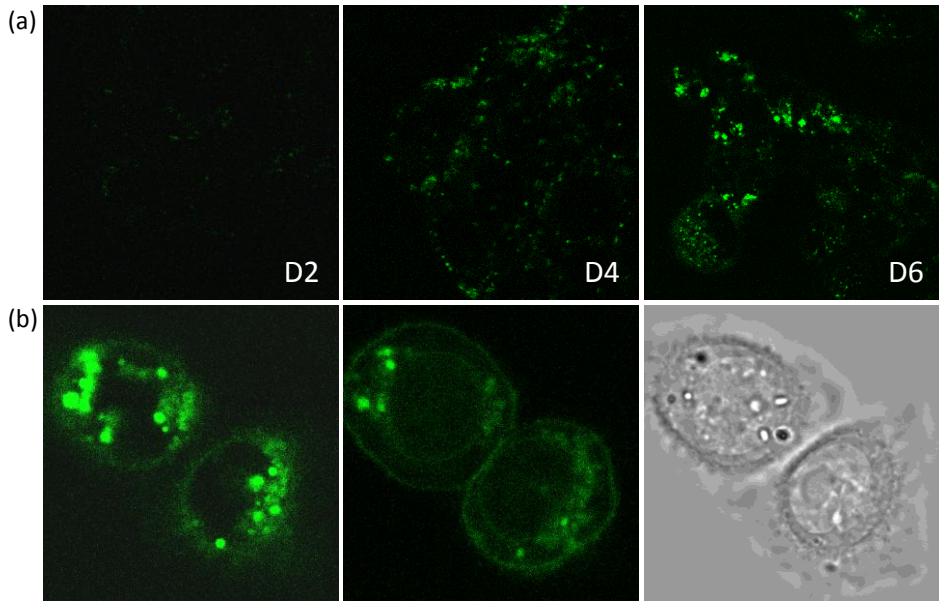

Figure 25. (a) Live cells incubated with complex (5µM) during 24 h, (b) From left: Cells incubated with D6 (5 µM) for 24h, the same cells after 10 min of illumination with 488 nm Ar-Laser and the transmission image.

Another kind of cells, neutrophilic lymphocytes, was used for cellular studies of the complexes. These cells are white blood cells purified from human blood and they are specialized to internalize and degrade bacteria or unknown substances. The result of the experiments show that D6 initially stains the cell membrane and upon laser illumination the complexes internalizes, see Figure 26. It was also clear that only illuminated cells were affected and thus the photoactivated uptake also occurs in this kind of cells.

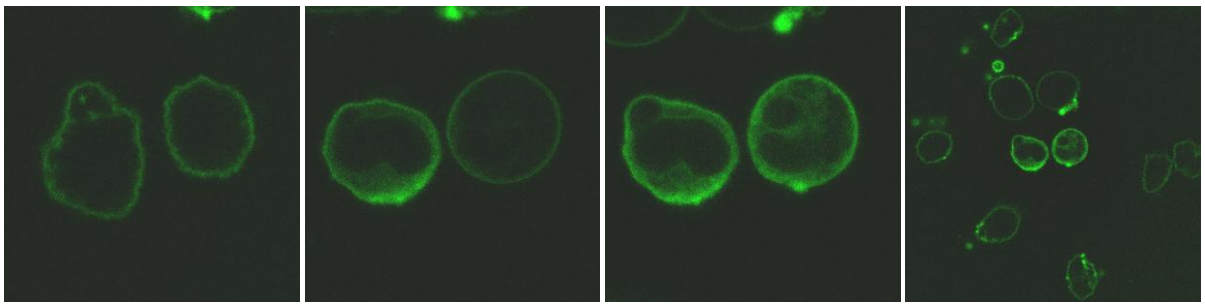

Figure 26. From left: neutrophilic granulocytes stained with D6 (2 µM), after 10 min of illumination, after 20 min of illumination and a zoomed out image revealing that the uptake only occurs in illuminated cells.

5. Discussion

The effect of small structural changes on molecular interactions and cellular localization are of interest in the research towards new cellular probes for imaging but also for development of new drugs. In this thesis the binding preference for RNA, DNA and membrane as well as the cellular localization of three lipophilic ruthenium complexes have been investigated.

The results show that the complexes have different binding preference and thus vary in cellular localization. From previously studies it is known that the more lipophilic complexes D6 and D4 prefer membrane binding while D2 favor binding to DNA in a mixture of DNA and membrane[10]. These preferences were confirmed in the experiments for this thesis which also showed that RNA cannot compete with the membrane binding for D6 and D4 and the DNA binding of D2. Although the binding is not the most favored, RNA binding was found for D6 and also to a smaller extent for D4 while the least lipophilic complex, D2, displays no or very week RNA binding. These results are consequent with the imaging of the cellular localization of the complexes where D2 stains the DNA in the nucleus but not the rRNA rich nucleolus while D6 dye the cytoplasm containing membrane and RNA. Emission of D4 is found both in the cytoplasm and in the nucleolus but also less intense in nucleus. Since there is both membrane structures and RNA in the cytoplasm it is hard to distinguish to what D6 and D4 actually are bound. Although the staining of the membrane probe, DPH, was not very detailed, the pattern of the nuclear envelope was clearly visible and this structure was also observed in the D6 and D4 staining. Since D4 is found in the nucleolus, it is probable that the complexes bind to both membrane and RNA. The absence of this staining for D6 might be due to high membrane affinity.

RNA has a hydrophobic interior, consistent with the two more lipophilic complexes binding to this nucleic acid and, as seen with emission spectroscopy, the three-dimensional structure of the RNA seems to have an impact on the complexes affinity. All complexes showed higher emission in rRNA compared to tRNA and the RNA oligonucleotide, which might be due to the complex three-dimensional structure of rRNA, rich in loops and double stranded parts. The binding was therefore suggested to be dependent on the loop structures but since D6 also showed equally intense emission in RNA oligonucleotide, which is an A-formed helix, the binding cannot be exclusively dependent on the loops. Unfortunately the binding mode of the RNA binding was not possible to investigate since the RNA could not be oriented in the flow cell for the LD measurements. This leaves questions about RNA binding unanswered. Do the complexes bind by intercalation in the double stranded parts of the RNA or are the complexes interacting in the grooves, loops or in hydrophobic parts so the dppz moiety is shielded from water?

From the gel electrophoresis experiments the RNA binding of the complexes were concluded to be weaker than the DNA binding. Prior to CYBR Green II staining, emission was detected at the same position in every well, including the wells with only RNA. Since the two RNA

types used migrate differently far, the emission of the complex should be at different positions at the gel. Additionally, there were no yellow bands at the RNA gel which was seen on the DNA containing gel. The conclusion was that the complexes did not migrate with the RNA and the detected emission was due to something in the RNase free loading buffer. Since the ruthenium complexes are positively charged and therefore would migrate in the opposite direction compared to the negatively charged nucleic acids the migration of the complexes with the nucleic acid relies on strong interactions. This requirement is fulfilled by the intercalation mode, proved for dppz, D2 and D4 in DNA by LD and CD, and because the RNA binding is much weaker the interaction might be of another character.

The LD and CD experiments performed in DNA gave similar pattern for all complexes but the magnitude of the signal was very small for D6, displaying that only a little amount of the complex binds by intercalation. The emission spectroscopy experiments also show that D6 itself is luminescent in the buffer. The absence of other molecules give the conclusion that the complex interact with itself, maybe by forming some kind of aggregates with the lipophilic alkyl ether chains together. The aggregation of this complex was concluded to depend on the salt concentration since the emission was not significant in lower salt concentration and the LD signal when bound to DNA was found to be higher at the lower salt concentration similar to the other complexes.

For emission spectroscopy it should be noted that it is not the actual binding that is detected, instead it is the change in micro-environment of the complexes. Thus the binding preferences are indicated by intensity and wavelength of the emission maximum and the change in these spectral properties when another component is added. Comparisons of spectra make it possible to distinguish if the complex is bound to one type of biomolecule or to both added components.

When designing a molecular probe for cellular imaging it is important that the probe show specific binding to the desired compartment. Additionally, it should also have low background luminescence, which is one property of these ruthenium complexes due to the light-switch effect. Another interesting photo physical property is the variation of the fluorescence lifetime depending on the surroundings of the complexes. By FLIM, the intracellular variation of the lifetime is possible to investigate independently of the intensity of the emission, after a threshold value is set. The obtained FLIM images for the different complexes display that the lifetime varies intracellularly with longer wavelength in the nucleus which is consistent with preliminary *in vitro* emission lifetime measurements. The lifetimes for D6 and D4 are in general shorter compared to D2 and the dppz complex. The lifetime calculation in the FLIM experiments is based on a reference with known lifetime and only references with similar lifetime will give a result close enough to the correct value. Since the lifetimes of the complexes in different environments are not fully investigated, the results of the FLIM experiments should only be used to probe differences. Note also the

presence of a high fluorescence lifetime in the nucleus of D6 which proves that this complex is also found in the nucleus although the intensity is too week for detection with CLSM system.

The cell membrane, the protecting barrier around the cell, does not allow the complexes to freely enter the cells as for fixed cells. The uptake is crucial for the function of both probes and drugs and therefore needs to be investigated. For the function of a drug aiming for killing cancer cells it would be enough just to surround cells with complex and illuminate specific cells with an intense light. Only illuminated cells would have a photoactivated uptake of the complex and these would soon die. Incubation of live cells in the dark, however, results in an uptake of the complexes which are seen as small punctuate structures in the cytoplasm. The mechanism is probably endocytosis, due to the large molecular structure and the charged ruthenium core which makes passive diffusion unlikely to occur. By the cytotoxicity test it is clear that the cells are still viable after 4 hours of incubation and thus dark incubation of cells with complex does not induce cell death under these conditions. The uptake of complexes in live cells shows the possibilities for development of probes and drugs with a similar structure but the complexes seem to be trapped in the endosomes. The complexes therefore have to be released from the endosomes to be able to stain the intracellular structures. The membrane of the endosomes was also found to permeabilize upon illumination which could be a way to release the complex into the cytoplasm. The staining after illumination of the endosomes is however weaker than for cells surrounded by complex because of the smaller quantity of complex encapsulated by the endosomes, which might not be satisfying for cellular staining.

Once inside the cell the complex distribute according to the affinity to the intracellular structures. Complexes with high affinity for DNA, for example D2, would be expected to interfere with transcription. By the *in vitro* transcription experiments the dppz complex is concluded to effects the transcription process and this outcome is also probable to occur in cells. The structural similarity and the proved intercalation of D2, D4 and dppz complex suggest that these complexes also would inhibit transcription. The more lipophilic complex is not found in the nucleus to the same extent and is not found to have as much intercalation binding mode in physiological salt concentration and thus are the most unlikely to inhibit transcription. The more lipophilic complexes could, however, be of interest for development of drugs with endoplasmic reticulum as target since ER stress also seem to induce cell death.

The findings in this master thesis may give valuable information for the development of new drugs and cellular probes. The complexes D2, D4 and D6 themselves are not probable drug candidates since there are many obstacles that have to be overcome for the cellular uptake and to gain the desired effect of them. However, by investigating the complexes and the change in properties due to the small change in lipophilicity may provide information that is of importance in development of new drugs which have structural similarities to these

complexes. D2, D4 and D6 are also shown to be promising probes, especially for fixed cells, with characteristic staining pattern depending on the lipophilicity of the complex.

6. Future work

Further studies of the three ruthenium complexes could focus on the binding mode of the RNA binding, differences due to stereochemistry, uptake mechanisms and cytotoxicity. To study the binding mode of the complexes bound to RNA, an approach to orient the nucleic acid would be important to develop. A longer RNA oligonucleotide, long enough to orient in the flow, or an appropriate stretched film technique could be alternatives to try.

The experiments done in this master thesis could also be repeated with the pure enantiomers of the complexes which would allow studies of the effect of the stereochemistry on binding, cellular localization and fluorescence lifetime.

Further, the mechanism of the observed photoactivated uptake could be studied. Since the mechanism is proposed to be dependent on oxygen radical formation the neutrophilic granulocytes, for which methods to study the radical formation has been developed, could be used to conclude whether this suggestion is correct or not. Also the mechanism behind the uptake for the dark incubated complex is interesting to study. There are commercial available endocytosis markers that could be used for this purpose.

It is not clear in what cytoplasmic structures that D6 and D4 accumulate. By higher resolution and better probes it might be possible to more exactly determine the cellular localization but since this approach might not give satisfying details other techniques should also be considered.

The toxicity of the complexes could also be further investigated with for example flow-cytometry. It would be of interest to compare the cytotoxic response of illuminated cells and cells kept in the dark.

7. Conclusions

From the investigations of the three lipophilic ruthenium complexes the following was concluded:

- The binding preference, and thus the cellular localization, of the complexes are highly dependent on the lipophilicity.
- D6 and D4 bind to RNA while D2 show no or weak RNA binding.
- The three-dimensional structure of the RNA has an influence on the binding of the complexes.
- In a mixture of DNA, RNA and membrane, D6 and D4 show preference binding to membrane while D2 binds to DNA.
- All complexes bind to DNA by intercalation like $[Ru(phen)_2(dppz)]^{2+}$.
- The DNA binding of the complexes is stronger than the RNA binding.
- The fluorescence lifetime of the complexes varies intracellularly with longer lifetime in DNA compared to the lifetime in membrane.
- *In vitro* transcription is affected by the DNA binding complexes.
- The lipophilicity of the complexes has an impact on the uptake in live cells.
- The photoactivated uptake also occurs in neutrophilic granulocytes.

8. Acknowledgements

I would like to express my gratitude to everyone that have helped me and supported me during my work with this master thesis. Thank you Frida Svensson for giving me this opportunity and for being an excellent supervisor and mentor. Thanks also to my examiner Per Lincoln for interesting discussion and for your support and to Bengt Nordén for your feedback.

I am also thankful to Kristina Fant who has shown me how to perform in vitro transcription, cytotoxicity tests and how to run gel electrophoresis and to Niklas Strömberg who in a very enthusiastic way showed how to perform FLIM experiments. Thank you Hanna Rydberg, Kristina Fant, Helen Åhman and Frida Svensson for the instructions and help in the cell lab.

Thank you Maria Abrahamsson for the help with lifetime measurements, Pär Nordell for showing me how to run kinetics, melting curves and for your ideas, Joakim Kärnbratt for introducing the time-correlated single photon counting instrument for me, Nils Carlsson, Erik Lundberg and Björn Åkerman for advice about my gel electrophoresis experiment and to the bachelor workers who helped me find stuff in the electrophoresis lab. Special thanks also to Lena Nyberg, Jan-Olof Dahlberg and Christian Brackmann who really tried to get the FLIM experiments to work.

Also I would like to thank all persons at the division for creating a joyful, harmonic and creative atmosphere and for all help with the instruments, interesting discussions and for being patient with the closed doors when I worked with RNA.

Last but not least I would like to thank my wonderful, understanding and interested partner Damir Džebo and my lovely family that have supported me through my education and carefully listened to me talking about totally non-understandable things.

List of References

1. Hurley, L.H., *DNA and its associated processes as targets for cancer therapy.* Nat Rev Cancer, 2002. **2**(3): p. 188-200.
2. Linder, S. and M.C. Shoshan, *Lysosomes and endoplasmic reticulum: targets for improved, selective anticancer therapy.* Drug Resist Updat, 2005. **8**(4): p. 199-204.
3. Fernandez-Moreira, V., F.L. Thorp-Greenwood, and M.P. Coogan, *Application of d6 transition metal complexes in fluorescence cell imaging.* Chem Commun (Camb), 2010. **46**(2): p. 186-202.
4. Clarke, M.J., *Ruthenium metallopharmaceuticals.* Coordination Chemistry Reviews, 2002. **232**(1-2): p. 69-93.
5. Erkkila, K.E., D.T. Odom, and J.K. Barton, *Recognition and reaction of metallointercalators with DNA.* Chemical Reviews, 1999. **99**(9): p. 2777-2795.
6. Friedman, A.E., et al., *Molecular Light Switch for DNA - Ru(Bpy)2(Dppz)2+.* Journal of the American Chemical Society, 1990. **112**(12): p. 4960-4962.
7. Friedman, A.E., et al., *Luminescence of ruthenium(II) polypyridyls: evidence for intercalative binding to Z-DNA.* Nucleic Acids Res, 1991. **19**(10): p. 2595-602.
8. Hiort, C., P. Lincoln, and B. Norden, *DNA-Binding of Δ-[Ru(Phen)2dppz]2+ and Λ-[Ru(Phen)2dppz]2+.* Journal of the American Chemical Society, 1993. **115**(9): p. 3448-3454.
9. Moucheron, C., *From cisplatin to photoreactive Ru complexes: targeting DNA for biomedical applications.* New Journal of Chemistry, 2009. **33**(2): p. 235-245.
10. Svensson, F.R., et al., *Lipophilic Ruthenium Complexes with Tuned Cell Membrane Affinity and Photoactivated Uptake*. 2010: Göteborg.
11. Svensson, F.R., et al., *Luminescent dipyridophenazine-ruthenium probes for liposome membranes.* Journal of Physical Chemistry B, 2008. **112**(35): p. 10969-10975.
12. Xu, H., et al., *Biophysical studies of a ruthenium(II) polypyridyl complex binding to DNA and RNA prove that nucleic acid structure has significant effects on binding behaviors.* J Biol Inorg Chem, 2005. **10**(5): p. 529-38.
13. O'Connor, N.A., et al., *A covalently linked phenanthridine-ruthenium(II) complex as a RNA probe.* Chem Commun (Camb), 2009(19): p. 2640-2.
14. Spillane, C.B., et al., *Dinuclear ruthenium(II) complexes as potential probes for RNA bulge sites.* Dalton Trans, 2007(45): p. 5290-6.
15. Alberts, B., et al., *Molecular Biology of the Cell*. 4th ed. 2002, New York: Garland Sicence.
16. Mathews, C.K., K.E. van Holde, and K.G. Ahern, *Biochemistry*. 3rd ed. 2000, San Francisco: Inc. Benjamin/Cummings, Addison Wesley Longman.
17. Watson, J.D. and F.H. Crick, *Molecular structure of nucleic acids; a structure for deoxyribose nucleic acid.* Nature, 1953. **171**(4356): p. 737-8.
18. *DNA structure*. 2010-03-22; Available from: http://www.chemistry.nmsu.edu/studntres/chem435/Lab4/dna4.gif.
19. *DNA 3D structure*. 2010-03-22; Available from: https://www.edulink.networcs.net/sites/teachlearn/science/Image%20Library/dna.jpg
20. *tRNA structure*. 2010-03-22; Available from: http://universe-review.ca/I11-21-tRNA2.jpg
21. Serianni, A.S., *16S rRNA secondary structure*, Chemistry and Biochemistry University of Notre Dame, Indiana.
22. *Mammalian cell*. 2010-03-22; Available from: http://media-2.web.britannica.com/eb-media/03/114903-050-CAFC50E4.jpg
23. Gennis, R.B., *Biomembranes - Molecular Structure and Function*. 1989, New York, USA: Springer-Verlag.
24. Vos, J.G. and J.M. Kelly, *Ruthenium polypyridyl chemistry; from basic research to applications and back again.* Dalton Trans, 2006(41): p. 4869-83.
25. Lincoln, P. and B. Nordén, *DNA binding geometries of ruthenium(II) complexes with 1,10-phenanthroline and 2,2 '-bipyridine ligands studied with linear dichroism spectroscopy.*

Borderline cases of intercalation. Journal of Physical Chemistry B, 1998. **102**(47): p. 9583-9594.
26. Holmlin, R.E., E.D. Stemp, and J.K. Barton, *Ru(phen)(2)dppz(2+) Luminescence: Dependence on DNA Sequences and Groove-Binding Agents.* Inorg Chem, 1998. **37**(1): p. 29-34.
27. Lincoln, P., A. Broo, and B. Nordén, *Diastereomeric DNA-binding geometries of intercalated ruthenium(II) trischelates probed by linear dichroism: [Ru(phen)(2)DPPZ](2+) and [Ru(phen)(2)BDPPZ](2+).* Journal of the American Chemical Society, 1996. **118**(11): p. 2644-2653.
28. Alderden, R.A., M.D. Hall, and T.W. Hambley, *The discovery and development of cisplatin.* Journal of Chemical Education, 2006. **83**(5): p. 728-734.
29. Chao, H., et al., *DNA interactions of a dinuclear ruthenium(II) complex bridged by 1,3-bis(1,10-phenanthroline[5,6-d]imidazol-2-yl)benzene.* Transition Metal Chemistry, 2006. **31**(4): p. 465-469.
30. Wilhelmsson, L.M., et al., *DNA-binding of semirigid binuclear ruthenium complex Δ,Δ-[μ-(11,11'-bidppz)(phen)(4)ru(2)](4+): extremely slow intercalation kinetics.* Journal of the American Chemical Society, 2002. **124**(41): p. 12092-3.
31. Ardhammar, M., P. Lincoln, and B. Norden, *Ligand substituents of ruthenium dipyridophenazine complexes sensitively determine orientation in liposome membrane.* Journal of Physical Chemistry B, 2001. **105**(45): p. 11363-11368.
32. Puckett, C.A. and J.K. Barton, *Methods to explore cellular uptake of ruthenium complexes.* J Am Chem Soc, 2007. **129**(1): p. 46-7.
33. Puckett, C.A. and J.K. Barton, *Mechanism of Cellular Uptake of a Ruthenium Polypyridyl Complex.* Biochemistry, 2008. **47**(45): p. 11711-11716.
34. Dobrucki, J.W., *Interaction of oxygen-sensitive luminescent probes Ru(phen)(3)(2+) and Ru(bipy)(3)(2+) with animal and plant cells in vitro. Mechanism of phototoxicity and conditions for non-invasive oxygen measurements.* J Photochem Photobiol B, 2001. **65**(2-3): p. 136-44.
35. Lacowicz, J.R., *Principles of Fluorescence Spectroscopy*. 3rd ed. 2006, New York: Springer Science.
36. Lincoln, P., *DNA Interactions with Chiral Polyaza-aromatic Ruthenium(II) Complexes*, in *Physical Chemistry*. 1998, Chalmers University of Technology: Göteborg.
37. Olofsson, J., *Intramolecular Electron Transfer in DNA and Ruthenium(II) Systems*, in *Chemistry and Bioscience*. 2004, Chalmers University of Technology: Göteborg.
38. Rodger, A. and B. Nordén, *Circular Dichroism and Linear Dichroism*. 1997, Oxford: Oxford University Press.
39. Oida, T., Y. Sako, and A. Kusumi, *Fluorescence lifetime imaging microscopy (flimscopy). Methodology development and application to studies of endosome fusion in single cells.* Biophys J, 1993. **64**(3): p. 676-85.
40. *Applications in Fluorescence Microscopy - Fluorescence Lifetime Imaging Microscopy (FLIM)*. 2009-11-03; Available from: http://www.olympusconfocal.com/applications/flimintro.html.
41. Semwogerere, D. and E.R. Weeks, *Confocal Microscopy*, in *Encyclopedia of Biomaterials and Biomedical Engineering*. 2005, Taylor & Francis.
42. Atkins, P.W. and J. de Paula, *Physical Chemistry for the Life Sciences*. 2006, New York: W.H. Freeman and Company, Oxford University Press.
43. *Oligoanalyzer 3.1* 2010-01-20; Available from: http://eu.idtdna.com/analyzer/Applications/OligoAnalyzer/Default.aspx.

Appendix

The spectra of D2 and D4 corresponding to Figure 14 are presented in Figure A1 and Figure A2. The results of the experiments with the different RNA types are all similar but the binding of D2 and D4 to tRNA and RNA oligonucleotide seems to be much weaker compared to rRNA binding, therefore only rRNA is used in the experiments presented below.

The least lipophilic complex, D2, has very high emission in DNA, with a maximum at 620nm, compared to the intensity in rRNA. The emission in DNA does not change much when rRNA is added and the small decrease seen in the spectra could be an effect of diluting. In contrast, the intensity is increased and the wavelength of emission maximum is shifted from 624 to 621 nm when DNA is added to D2 in rRNA, indicating a stronger affinity for DNA than rRNA. In liposomes the emission is much lower than in DNA and for a mixture of rRNA and liposomes the complex seem to bind to liposomes but also to rRNA to some extent due to that the wavelength for the mixture (643 nm) is in between the emission in pure rRNA (624 nm) and liposome (645 nm), see Figure A1.

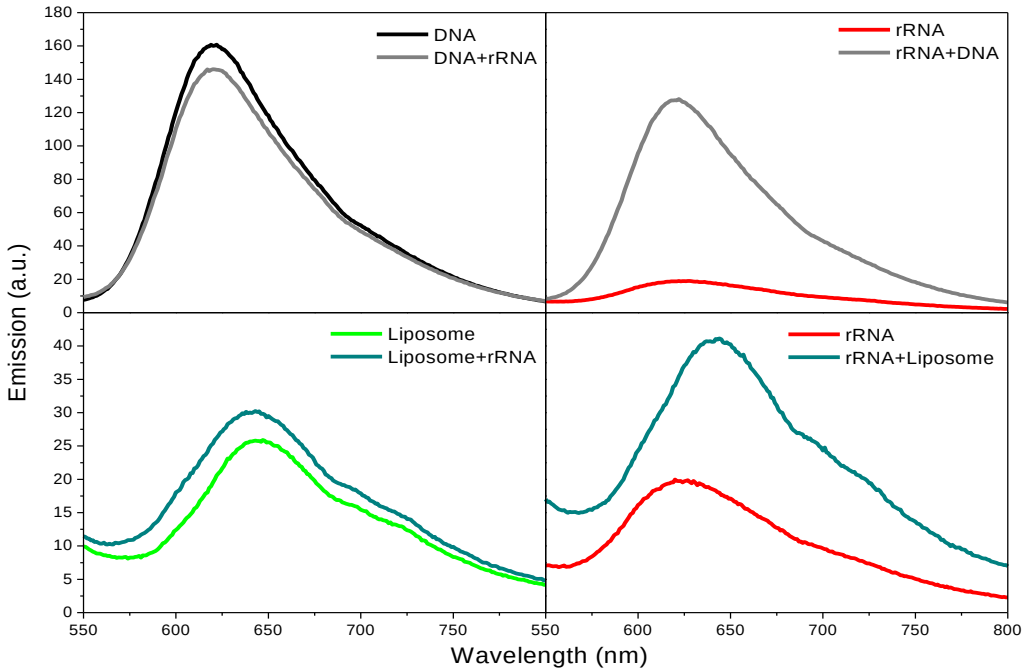

Figure A1. Emission spectra of D2 (2 µM) in pure DNA (40 µM bases,) rRNA (40 µM bases) or liposome (200 µM) and the spectral change upon addition of rRNA, DNA or liposomes are displayed.

The emission for D4 in DNA is also intense (maximum at 620 nm) and upon addition of rRNA the emission is decreased. This effect is more apparent compared to the corresponding spectra for D2. For the opposite experiment where DNA is added to an rRNA sample the emission increases and the wavelength of the emission maximum is shifted to 621 nm from 624 nm. This indicates a preference for DNA binding of the complex. The spectra for D4 in liposomes does not change when rRNA is added while the spectra in rRNA changes towards liposome binding, concluded from the wavelength shift, when liposome is added, see Figure A2.

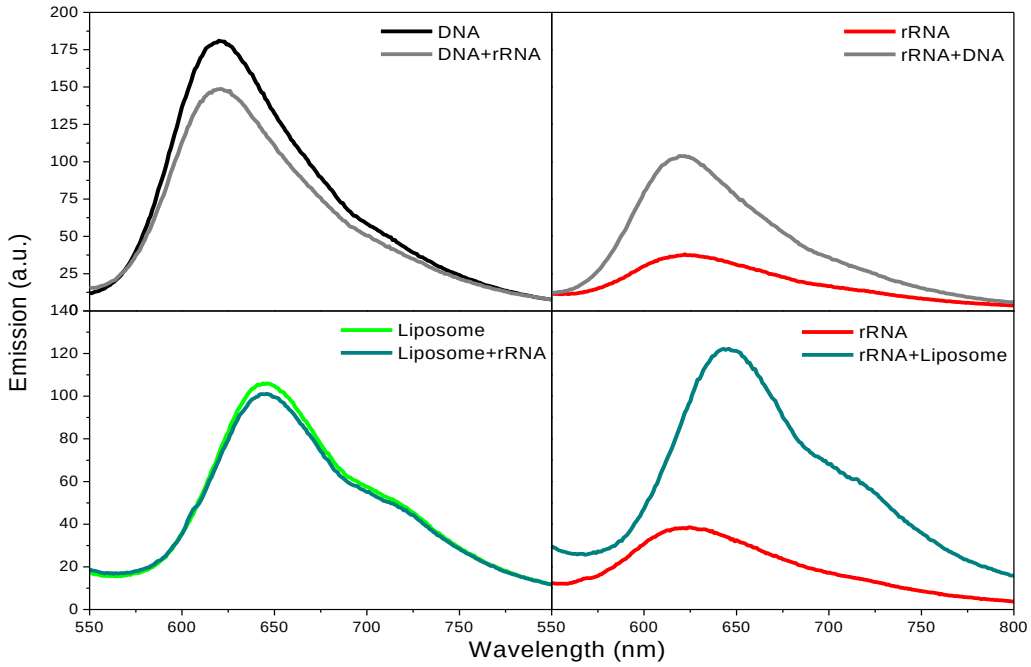

Figure A2. Emission spectra of D4 (2 µM) in pure DNA (40 µM bases,) rRNA (40 µM bases) or liposome (200 µM) and the spectral change upon addition of rRNA, DNA or liposomes are displayed.